

Answers to RC1

RC1: The paper “Permafrost distribution in steep slopes in Norway: measurements, statistical modelling and geomorphological implications” by Magnin et al. presents a new rock permafrost model for mainland Norway and draws conclusions of permafrost distribution in rockwalls on current rock instability and landform development. The authors installed more than 25 rock temperature loggers in 8 key regions and used a sophisticated model approach to upscale their findings on the rockwall thermal regime into a regional rock permafrost model. Rock permafrost in Norway is responsible for a large number of rock instabilities that currently threaten infrastructure and inhabitants.

Authors’ answer: *At the current stage, the role of permafrost as a main cause of rock wall instability in Norway is not clear, and neither the authors nor other studies clearly claim that permafrost is responsible for a large number of rock instabilities, especially in Norway. Our study does not draw any conclusions “on current rock instability and landform developments”. Our conclusions are all related to the outcome of the rock wall logger analysis and upscaling of the data to a national scale using statistical methods (see P15 – L5-29 of the submitted version: there are no conclusion points stating about rock slope instabilities and landforms).*

RC1: In the past, these instabilities caused hundreds of deaths and the knowledge of rock permafrost distribution as provided by this paper is required to mitigate ongoing and future landslide hazards and risks. Therefore, the importance of this work is very high. Unfortunately, the link of permafrost distribution to rock instabilities is poorly addressed,

Authors’ answer: *Yes, this is right. But, as mentioned above, the goal of this paper is not to address the link between permafrost and instabilities. This is not feasible with the existing data and our approach. However, we believe that our study is an essential step towards assessment of the link between permafrost and instabilities, and this could be addressed in future studies.*

RC1: ... the use of chosen parameters of the model are incompletely explained, ...

Authors’ answer: *in the revised version we added a paragraph in the introduction about rock slope permafrost modelling which explains our choice in terms of model parameters.*

RC1...results are insufficiently presented and compared to non-connected landforms (moraine-derived rock glaciers) instead of existing instabilities.

Authors' answer: Since we do not address the role of permafrost for landform developments and rock slope instabilities, we have not shown anything about possible relations pointed out by RC1 in our results. We included the mentioned points in this study with the intention to show that our results could be used to address landforms and instabilities and therefore hint at possible applications to address geomorphological questions in our discussion. In addition, we never use the term "moraine-derived" for the rock glaciers inventory that we introduce in the manuscript.

RC1: In addition, the reader needs knowledge on Norwegian locations to understand the research set up.

Authors' answer: Yes, we noticed indeed that some terms we use may confuse some readers not familiar with the Norwegian settings and that we also referred to locations that are not clearly displayed in any of the maps. We have corrected this following the details comments. We have removed specific terms that were not essential to the study (such as "Scandes") and made sure that we only referred to locations displayed in Figures.

RC1: In current state, the paper focuses on permafrost and lacks on geomorphology and would be better suited for a journal focusing on periglacial phenomena than Earth Surface Dynamics. However, a revision which address the shortcomings would improve the manuscript and the suitability.

Authors' answer: As mentioned above, here we strongly disagree with RC1, based on our introductory statements above. We notice also that neither RC2 nor the handling associate editor gave us a similar opinion.

RC1:

1) Link between permafrost and rock stabilities. Permafrost affects rock stability, however, this effect can be both positive and negative, thus, permafrost affects driving and resisting factors as previously discussed Krautblatter et al. (2013) and Draebing et al. (2014). Permafrost aggradation for example following the LIA causes cryostatic pressures (Wegmann et al., 1998), however, this does not provoke ice segregation and large rock slope failures as suggested by the authors. Ice segregation can be amplified by permafrost when active-layer thaw increase rock moisture that can migrate towards the freezing front at the top of the permafrost as identified by Murton et al. (2006). However, this effect is limited to the upper 20 m of rock depth (Krautblatter et al., 2013), thus, the normal load of the overlying bedrock would counter the effects of ice pressure. Therefore, ice segregation cannot cause rock slope failure with shear planes below 20m depth. The authors are not addressing further effects of permafrost on instability. The

instability of permafrost rockwalls is also affected by active-layer thaw that can cause small-scale rockfall as conceptually discussed by Draebing et al. (2014) and derived from rockfall inventories by Ravanel et al. (2010; 2017). Permafrost warming and degradation increase instability as mechanically described by Krautblatter et al. (2013) and can result in an increase of rockfall activity (Ravanel and Deline, 2010). Due to these findings, several authors discuss a connection between rock slope failures and quaternary climate fluctuations in Norway (Hilger et al., 2018; Matthews et al., 2018). The authors should include these findings in their introduction and in the discussion of their results. Beneath these permafrost effects, rock slope stability is controlled by paraglacial effects which are non-glaciated processes conditioned by former glaciation as the authors mentioned. McColl (2012) and McColl and Draebing (2019) recently reviewed paraglacial effects on rockwall stability and connection to permafrost dynamics. Oversteepening of rockwalls results in stress redistributions and can prone rockwalls towards instability. Thus, areas affected by permafrost are very often also affected by current or former glaciation, paraglacial and periglacial effects are hard to decipher. This can become even more complicated as paraglacial adjustment can work over more than one glacial cycle (Grämiger et al., 2017). The author introduce vaguely paraglacial effects without including any up-to-date literature or discussing a potential influence. The problem of deciphering periglacial and paraglacial processes should be addressed in the discussion.

Authors' answer: Thank you for the detailed comment. We re-wrote the paragraph to make it more accurate and aligned with the relevant literature (see the revised introduction), including some of the points here mentioned. However, the given explanation here goes far beyond our paper's concern, and we kept a concise paragraph. Additionally, we didn't not address the following comment: "problem of decipher periglacial and paraglacial processes". This is worth a paper alone, and we can have a long discussion about "periglacial" and "paraglacial" and other semantic issues, and as mentioned in the beginning, we think this is not the objective of our manuscript.

RC1:

2) The modelling approach The authors a priori chose a slope angle threshold of 40° to identify steep rock slopes. There is no geomorphic argument why this threshold is chosen. Previous models by Hipp et al. (2014) and Steiger et al. (2016) chose a threshold of 50° and 60° for steep rock slopes in Norway. Before extrapolating the results to entire Norway, the authors should try to evaluate their threshold. They can map rockwalls from orthophotos for small areas or data subsets and compare them to rockwalls derived by their threshold approach to test the sensitivity of their model.

Authors' answer: Thank you for this comment, which is totally correct. Depending on the study such threshold varies because there is no strict DEM slope value above which a real-world steep slope is accurately represented on a DEM. Furthermore, it does not exist a scientifically-based threshold. The main characteristic of rock wall permafrost is the absence of perennial, continuous and insulating snow cover in winter. However, as mentioned in this comment, this can happen locally, not continuously in space, in slope up to 75°. If we take slope > 75° on the DEM we use, there will be almost no slopes left, because as all DEMs, it underestimates slope angles due to data interpolation. In a dem, true vertical doesn't exist, as the walls have a certain horizontal extent, even if they are vertical. In addition, a systematic comparison of a DEM slope angle to the real-world slope angle is not feasible over a whole country and possible comparison at the local scale will be only valuable for the considered area due to varying quality of the DEM over space. It has to be noted that in the case of vertical walls, the aerial fraction within a km² would be zero, even though it could still have lots of walls in this area. We therefore decided 40° as it is rather conservative: it includes mid-steep slopes more or less affected by snow but does not exclude steep slope areas by taking a higher slope angle. This involves that some slopes considered in our study may be affected by snow deposit and this is why we provide interpretation-keys together with the permafrost probability value. In the current state, it seems like the best possible option and we have explicated this choice and its limitations in the revised version. See 2nd paragraph of section 3.4 in the revised version.

RC1: Also they could compare their derived rockwalls with the location of instabilities mapped by Oppikofer et al. (2015).

Authors' answer: Yes, this would be a nice addition. Unfortunately, this is not feasible: see P13 L30-35 and P14 L1-2 of the submitted version. It is explained that the instability database gathers many types of instabilities (not only steep rock slope instabilities), that they are inventoried by a point at the middle of the slope (not necessarily in its steepest part). Therefore, we did the best we can, taking into account data limitations, which is still relevant to hint at possible research perspectives.

RC1: The rock temperature loggers are installed following the approach by Gruber et al. (2004) which choose the steepest part of the rockwall to limit effects of snow accumulation. Therefore, the setup excludes snow cover, which can be present even in rockwalls with a slope angle up to 75° (Haberkorn et al., 2015a; Haberkorn et al., 2015b; Haberkorn et al., 2017; Phillips et al., 2017). Figure 5 shows that large rockwall areas are covered by snow cover. A coarse DEM with a resolution of 10 m will smooth out ledges that enable snow accumulation (Draebing et al., 2017; Haberkorn et al., 2015a), therefore, the chosen resolution will limit the effects of snow cover. Snow cover is also highly heterogeneous in space and time, which makes it

very difficult to include in modelling approaches. However, the author should mention and discuss this shortcoming of the model resulting from chosen logger locations and DEM resolution.

Authors' answer: Again, RC1 rises a valid and important point. In a local scale, snow is an important moderator of ground thermal regime even in steep rock walls with ledges, and overall slope ruggedness. However, in our regional approach, whatever the DEM resolution the snow effect will not be accounted for. Independent of the DEM resolution, the model is either able to consider snow (e.g. physic-based model for site scale), or the model does not account for snow, such as in our approach (statistics, appropriate for large spatial coverage) and in that case the capability of the DEM to represent ledges has no influence. We did mention and discuss the lack of consideration for snow effect in our study, see in the explanation of our modelling approach P7 L30-32 and P8 L1-6 and in the discussion P 12 L3-8 and 13-17. This is why we provide interpretation-keys with the probability map, to consider the snow effect as at the current stage, this is the best we can do for such statistic-based approach. It has to be noted that the Norwegian conditions are very different than the conditions in the Alps, and that studies conducted on snow control in the Alps cited in this comment are not strictly transferable to the Norwegian case. Indeed, due to the dominant control of solar radiation on the permafrost distribution and dynamics in the European Alps, the snow albedo strongly controls the snow effect, especially on South faces (Magnin et al., 2017b; Haberkorn et al., 2017). In Norway, the snow control on steep rock faces has not been investigated yet quantitatively, and therefore we limit our explanations and discussion to what is possible to say. We better explained how we handle the lack of consideration for snow in the revised version, first in the introduction (3rd paragraph), section 3.1 2nd paragraph, First 3 lines of section 3.3. section 3.4 2nd paragraph, section 3.5 3rd paragraph, section 5.2 2nd paragraph.

RC1: In their model, the authors simulate PISR using GIS. It is unknown which latitudinal location and the time period they chose to run the PISR algorithm provided by ArcGIS. Solar parameters show large changes between North and South of Norway and model results should reflect this. The author should therefore provide more information on the modelling approach and how they incorporate differences within their data set.

Authors' answer: We provide details (including time period and time resolution) about the PISR calculation in P6 L24-35, P7 L1-3 and 5-7. The latitude is intrinsic to the DEM, therefore for each grid cell the specific latitude is attributed and considered in the calculation. This is why there are great difference between Northern and Southern Norway, and that this is reflected in our results: P9 L14-35, P10 L 1-6 for example, based on Figure 9. This issue is also further discussed P 11 L21-35.

RC1: The authors classify permafrost occurrence based on bedrock setting. They refer to Figure 5 where they highlight three areas and suggest different fracture properties in these areas. From the photo alone, fractures or degree of fracturing is not visible. It remains unclear where the fracture information comes from for e.g. local sites or even entire Norway. However, the authors use this information to classify permafrost into isolated, sporadic, discontinuous and continuous permafrost based on a permafrost classification scheme for the Arctic. In Alpine areas topography has strong control on permafrost distribution and the use of this scheme is limited. The same authors use a permafrost probability approach in the Mont Blanc Massif (Magnin et al., 2015; Ravel et al., 2017), which is better suited. The authors connect this scheme somehow to slope ruggedness and fractures but it is completely unclear where they derive the information from necessary for the classification. If you apply the classification to the rockwall in Figure 5 and assume the fracture properties are correct discontinuous permafrost can be located in direct proximity to isolated or spontaneous permafrost. It would make more sense to model rockwall permafrost and compare every pixel to its neighbouring pixels to identify isolated, sporadic, discontinuous and continuous permafrost.

Authors' answer: *In this case we think RC1 may have misunderstood. We classify permafrost occurrence according to permafrost probability: P7 L22-25 of the submitted version and also see Figure 9 for example. We refer to Figure 5 to give an example of how to interpret the permafrost probability according to the bedrock settings. It is the map user who is supposed to interpret the map according to the bedrock settings in his/her area of interest, and Figure 5 only gives an example of possible interpretation according to the state of the art knowledge. However, we admit that using the term "fractured" might be confusing as we associate to surface slope angle and ruggedness, which are not strictly linked. We therefore re-wrote the legend of Figure 5 to avoid such confusing terms and developed our conceptual approach to interpret the permafrost probability map in more details in the 2nd paragraph section 3.5. Furthermore, the studies referred in this comment use a similar approach as in this paper: calculation of a statistical distribution first, and interpretation afterwards. But to be precise, in our study we use a slightly different approach than in the referred studies, we calculated an index while in the present paper we calculate a probability. In both cases, our approach is based on the state of the art relevant for the investigated area.*

RC1: Rockwalls are not uniformly distributed in Norway and conclusions on rock permafrost occurrence cannot be used without normalization. Differences between East and West Norway are caused by a decrease of rockwall occurrence and not permafrost occurrence. Other periglacial landforms are abundant in the east and the authors cannot conclude on permafrost distribution without normalization.

Authors' answer: We think that this is a highly relevant idea, but the argumentation merely denies what we wrote in the submitted version: "Differences between East and Western Norway are caused by a decrease of rock wall occurrence, not permafrost occurrence". This is exactly what we meant P11, L30-32: "The number of permafrost observations decreases with continentality as most of the rock walls are found close to the coast". Maybe the fact that we did not precise "the number of **rock slope** permafrost occurrences" have confused RC1 who thought about "permafrost observations" in general? As it is our results section focusing on rock slope permafrost we thought it was not necessary to mention "rock slope" but we added this precision in the revised version.

Additionally, normalizing the results will fade the topographical control (rock wall occurrences and elevation) on our results, which is definitely not what we wanted to show. We think that this is very important to show that permafrost distribution is also a results of the topographical settings, and this is why we preferred to show all observations in Figure 10 for example rather than normalized results. In this study, we do not use rock walls as permafrost indicators, which in that case would make sense to normalize the results before using rock walls to map permafrost distribution. And we also explain in the submitted paper that the very few number of rock walls occurrences in Eastern Norway makes a statistical analysis poorly relevant, including normalization. We chose what we think is the most appropriate way to express our results and therefore avoid normalization.

RC1: Comparison to rock glaciers and the use of instabilities The authors compare their permafrost distribution to other landforms such as rock glaciers and found a strong local connection to moraine-derived rock glaciers. Areas affected by rock permafrost are very often previously glaciated and inhabit other periglacial and glacial landforms. Permafrost rockwalls can produce material that can accumulate on snowfields and with time, the material can develop into a talus-derived rock glacier. The permafrost develops when debris-covered snow develops into ice via ice metamorphosis. The permafrost in the rock glacier has no causal connection to permafrost in the rockwall. Moraine-derived rock glaciers are developed from creeping former dead ice and is more connected to previous glaciation. Due to a lack of connection, a comparison makes no sense.

Authors' answer: Again, we think RC1 has misunderstood something. Our paper doesn't claim a "strong connection" or causal between rock glaciers and rock wall permafrost. We do not mention the rock glacier origin, and the term "moraine-derived" rock glaciers is not used at all in our paper. Our paper simply shows in sect. 5.4 that mapped active rock glaciers often are surrounded by rock wall permafrost. It therefore suggests to explore the link between permafrost in debris slopes and in rock walls. Our statement with this respect is as follows:

“This underpins the interest for studying the connection of permafrost rock walls and adjacent landforms which so far, to the author’s knowledge, has not been directly addressed. Indeed, permafrost dynamics can influence material supply pattern to these landforms, as e.g. frost cracking varies greatly within and without permafrost environments (e.g. Hales and Roering, 2007).”

RC1: The author should focus on their objectives and present directly from the beginning the Norwegian rock instability inventory by Oppikofer et al. (2015). They should test if their threshold-derived rockwalls include all instabilities. Furthermore, they should compare their permafrost distribution to the location of instabilities. Can you develop a relationship based on your data?

Authors’ answer: And again, we think RC1 has misunderstood, which of course could be our wording or language. We have therefore clarified our paper’s objectives in the title and in the introduction to avoid such misunderstanding are our objectives are definitely not to present the rock instability inventory and its link with permafrost as claimed by RC1. See other comments above the limitations of such study in the current state. Defining a relationship between permafrost distribution and the slope instabilities inventory is not feasible in the current state.

RC1: What would be interesting is to model future permafrost distribution as previously done by Hipp et al. (2014) by using temperature increase scenarios. The authors can compare future permafrost distribution to slow creeping rockslides (e.g. Jettan) and other instabilities in the inventory and can draw conclusions of permafrost degradation on potential instability sites. The map could identify hot spots of future rock slope failures, which can be used for hazard mitigation such as planning or zoning. This would be of more interest than comparing permafrost distribution to other periglacial landforms.

Authors’ answer: Yes, this would indeed be interesting. It is a.o. therefore we wanted to publish our results as a base line of rock wall permafrost distribution in Norway. Like in Hipp et al., (2014) we of course work on calibrating transient heat flow models for the study sites. Until now we have given priority to look on the thermal history rather than the future, soon to be published in a PhD theses and papers therein. We certainly will work on the future impact, but probably more site specific. However, this is not the objective of this study.

RC1: In summary, this paper can be a very important contribution to Earth Surface Dynamics if linkages between permafrost and instability are improved and coherently discussed. The model set up should be better explained and sensitivity of the rock slope angle threshold evaluated. The paper should focus more on rock wall

instabilities, thus, the Norwegian landslide inventory provides a unique dataset and comparison to current and future rock permafrost distribution would provide valuable information for geomorphologists but also for hazards mitigation by the managing authorities.

- 5 **Authors' answer:** *In the revision we better explained our model set up, also following comments from RC2. We better detailed the choice of loggers' locations (section 3.1, 2nd paragraph) and slope threshold choice (see answer to former comment about this point). Concerning the relationship between permafrost and rock wall stability, see our introductory comments to this reply.*

10

Answers to RC2

- 15 **RC2:** The manuscript presents an important study for a better understanding on how permafrost is distributed within rock walls. It relies on a high number of rock temperature data and the outcomes of the study are significant. The manuscript is rather well written, but sometimes the text is a bit confused and thus not always easy to follow. The results are generally well discussed, and the last section of the discussion presents interesting and original reflections. However, the manuscript contains some issues, the most important one being that the model is not enough clearly explained, as for the model parameters. The way on how the RST data were used to calibrate the model must be much better explained. Some figures must also be improved, because not enough clear or not enough explained. For non Norwegian people it is sometimes difficult to follow. I present here after some general comments, and then more specific comments.

- 20
- 25 **Author's answer:** *We thank reviewer 2 for insightful comments, and try to address the points raised above. Details of our revision are given in the following.*

- RC2:** In the Introduction, a chapter on the different models used hitherto to predict the occurrence of permafrost in rock walls is missing. What is the story of the research in this field ? Which models were used ? Where ? etc.

30

Author's answer: *We have added a paragraph summarizing the history of rock slope permafrost studies, with a specific focus on statistical approaches as this allows better introduction of our study.*

- 35 **RC2:** The method used to predict MARST must be better explained. It's not clear how the authors used the measured MARST to predict MARST. In the equation (1), MARST is predicted from PISR and MAAT only, and I guess the relation between MARST and PISR / MAAT is expressed in the coefficients b and c, but it's not expressively shown. So this section is a bit confused and needs then additional details.

Author's answer: We have provided more information about the modelling approach, by providing first the statistical basis of multiple linear regression model as a first Equation, and explaining how we link the 3 variables. See Lines 1-6 P6 of the revised version. Then, concerning the statistical significance of each coefficients, this is provided in section 4.1 and we can not give such information in the methods as this is purely results of our study.

RC2: The permafrost occurrence is defined when the rock surface temperature is $\geq 0^{\circ}\text{C}$. This is true for permafrost in equilibrium with current climate conditions, but permafrost can be present at depth even with positive surface temperatures, due to thermal offset and thermal inertia. In this case permafrost is not in equilibrium with the current conditions. This must be taken into consideration. Obviously it is, since MAAT is calculated for the period 1981-2010, but this must be better explained.

Author's answer: Yes, this is entirely true and needs to be explicitly provided in the interpretation of our permafrost probability map. We therefore added a few explanations about this point in Section 3.5 in order to refine the interpretation keys.

RC2: The concepts of "lower limit of permafrost" and of "lowermost observations of the lower altitudinal limit" (LAL) must be better defined. At this stage the difference is not clear it is not evident to understand why the second was introduced.

Author's answer: Yes indeed. We were not very clear with the use of these concepts. In section 4.2 we introduce the concept of LAL, and avoided the use of the «lowermost observation of the LAL».

"In Figure 9 we display the distribution of the lowest occurrence of each permafrost class (i.e. the distribution of the occurrences of probability 0.1, 0.5, and 0.9) according to elevation and latitude. We refer to these lowest occurrences as the "lower altitudinal limit" (LAL) of each permafrost class."

And we replaced the «lower limit of permafrost» by the «LAL» as it is basically the same concept, but that we referred to in a different manner in the results and discussion sections.

RC2: In the discussion chapter, section 5.3 is very difficult to follow. It contains many descriptive parts that compare permafrost elevation in north and south faces with more gentle slopes in specific locations, which are not always visible on Fig. 11. In the end it is very difficult to capture the main message. I suggest to reorganize the text, to be more systematic in the comparisons, and also more synthetic.

Author's answer: We re-wrote this section following this comments. We removed parts of the description to focus more the key message and hope it is clearer in the revised version.

RC2: Regarding FigureS3, there are huge differences between the outcomes of the two models. This must be addressed in the text.

Author's answer: When re-writing the section, we have given explanation to these differences. See at the end of the 1st paragraph of section 5.3.

RC2: The question of the influence of continentality on the permafrost occurrence and lower limit should be also addressed more largely, and not only for Norway. Some studies (e.g. Sattler et al. 2016 for permafrost in New Zealand) showed that permafrost may reach lower elevations in more humid locations than in continental ones.

Author's answer: Thank you for reminding us this relevant study from Sattler et al. (2016). In the revised version we reinforced our argumentation on cloud cover effect of maritime areas as suggested in this study in section 5.2, but we did not extend the discussion on the continentality too much in section 5.3 because it will center the discussion on gentle slopes permafrost while we focus on steep rock slopes.

RC2: Regarding the form, in the introduction especially there is a lack of transitions between some sentences. It is often a juxtaposition of sentences, without any link. Ex. .1, l.30, P.2, l.13, l.20. The text contains also many typos, especially in the Discussion sections. I noticed some in the specific remarks below, but in the end, I renounced todo it for all the manuscript. So please check them carefully.

Author's answer: As mentioned in the introductory words, we re-wrote the introduction and hope it is better organized and more logic. Thanjk you for noticing some typos, we thoroughly checked the entire revised version before submission.

10 **Specific comments:**

P.2, l.14. Why "in the" ? → *that was a mistake, corrected*

P.2, l.16. Rock fall and rock avalanches are not agents, but processes, or events. → *Right, corrected*

15 P.2, l.22-34. How many of these 800 events triggered from potentially permafrost-affected rock walls ? → *this is unknown.*

P.3,l.12. Geologists are also interested in the influence of permafrost on rock wall stability, so choose a more general term than "geomorphologists". → *Right, we replaced by «earth scientists»*

20 P.5, l.2. This kind of sentence should be moved in thestate-of-the-art section in the introduction → *Done, we merged it with the new paragraph explaining the state of the art in terms of rock wall permafrost modelling.*

p.5, l.3. Add a reference. → *This is merged with the state of the art in the introduction, with relevant references in the revised version.*

25 p.5, l.8. "therefore"means that from the former line we can directly derive the equation presented. This is not so obvious. Please be more precise. Then I don't understand how the coefficientsa, b and c are calculated. → *in the revised version we provide the statistical basis of multiple linear regression models and explicit how the coefficients a, b and c are calculated in section 3.3 which is the appropriate section for such explanation.*

30 p.5, l.9. It is unclear if the way to predict MARST is original in this study of if it has been already proposed in former studies. → *We have elucidated that comments with the new paragraph in the introduction, the new lines introducing section 3.2, and added also some details in section 3.3 which is the most appropriate to give such information.*

p.5, l.16. The coma must be moved after "model" → *done*

p.6, l.14. Unclear to what correspond those 85 MARST points.Due to different years ? → *yes, we stated it explicately in the revised version.*

35 p.6, l.24 and following. It's unclear which DEM resolution the authors choose : 1 m or 10 m ? → *At this line, the different DEMs have not been introduced yet. They are introduced l27-29. Then we explain which are possible criteria to choose the DEM we use (hillshading effect or better representation of the real-world topography). Then, L34-35 and P7 L1-2 we explain that finally, we chose the DEM based on the best match with real world conditions at location of RST loggers.*

- p.7, l.11. Fig 4, not 5 → *True, we changed it*
- p.9 l.18. The “LAL” is not easy to understand. What is the difference with the lower limit of permafrost ? Why defining this new concept ? → *See answer to the general comment.*
- 5 p.10, l.3-6. The lower limit of discontinuous permafrost must be better defined (see my general comments). → *Yes, we improved it, see answer to former comment.*
- Fig. 10 does not show between 0°C isotherm and latitude. → *True; we actually kept these sentences from a former version where we fitted a linear regression between the LAL of discontinuous permafrost and latitude, but finally removed it because it was not bringing something completely new compared to Figure 9. We removed these sentences in the revised version.*
- 10 In the same section the decrease of the lower limit of permafrost northwards appears to be more pronounced than the decrease of the LAL. How can the authors explain this ? And again, it is really not easy to follow, the difference between the two concepts being not clear. → *Yes, regarding this comments, it is clear the the concept was not clearly explained and this is why such a question arise. With the explanation at the beginning of the question, such question should not arise. The Lower limit of permafrost is the same as the LAL, and this LAL decreases northward for each permafrost class.*
- 15 p.10, l.8. Show on a map where the Caledonides are. Then, since most of the rock walls are located in the interior mountain massifs they should also be located in more continental conditions. Thus there is a problem of logic in this sentence. → *Yes, this is true that this sentence is not logic. We rewrote it to avoid confusion.*
- 20 p.10, l.26. Check the syntax. → *Done, we rewrote it.*
- p.11, l.8. . . . 2 m AT. First, AT must be spelt out here (the reader may have forgotten the meaning of the acronym). Second, from where comes this 2m AT ? I did not find it in the method section. → *we wrote air tempertaure with plain text and removed the «2 m» as this was not a relevant detail to understand the study and refers to details of Lussana et al. work.*
- 25 p.11, l.14-15 : Fig.13 (there is no Fig., 15) → *right! corrected*
- p.12, l.3. Remove the coma after “both”. → *Done*
- p.12, l.5-8. A bit confused. Do not put such long explanations into brackets. → *We rewrote the sentence.*
- 30 p.12, l.26. Both figures 10 and 13 do not show this decreasing elevation of permafrost across continentality. → *This is true that for Figure 13, the link with continentality is less evident and we rewrote the text accordingly.*
- Fig. 5. Indicate in the caption the significance of the yellow dots. → *Done*
- 35 Fig. 9. How can the authors explain the plateau between 62°N and 66°N ? → *This is due to rock wall distribution, and air temperature. We mentioned it in the submitted version P9 L23-24 but rephrased it in the revised version to point ut out clearly.*
- Fig. 9 and 10. Please align the grid on the labels of the Y axis. → *Done*

Fig. 11. Please explain somewhere why the threshold 0.5 is used to create the CryWall map. In the caption indicate what show the squares and the yellow circles. ➔ *Done*.

5 Fig. 12. The maps are quite difficult to read. The legend must show the 6 colors present in the map. I suggest to make the differences between the two used models clearer, by having more distinct colors. Same remark for Fig. S3 and S5. ➔ *Here we chose to use the same color range for both models because we want to make the different permafrost classes comparable between the gentle slope permafrost model and the rock wall permafrost model (CryoWALL map). By using different colors, it would be harder to directly compare the permafrost classes of the 2 maps. Thus, this is not 6 colors but 3 colors with different transparency. Instead of changing the colors, we have improved the legend as this is true that this was not clear and lead to confusion. We did the same for Fig. S1.*

10

Permafrost distribution in steep rock slopes in Norway: measurements, statistical modelling and implications for geomorphological implicationsprocesses

Florence Magnin¹, Bernd Etzelmuller¹, Sebastian Westermann¹, Ketil Isaksen², Paula Hilger^{1,3}, Reginald L. Hermanns^{3,4}

¹ Department of Geosciences, University of Oslo, Oslo, 0316, Norway

² The Norwegian Meteorological Institute, Oslo, 0313, Norway

³ Geohazards and Earth observation, Geological Survey of Norway, Trondheim, 7040, Norway

⁴ Institute for Geoscience and Petroleum, Norwegian University of Science and Technology, Trondheim, Norway

Correspondence to: Florence Magnin (florence.magnin@geo.uio.no)

Abstract. Permafrost in steep rock slopes has been increasingly studied since the early 2000s in conjunction with a growing number of rock slope failures, which likely resulted from permafrost degradation. In Norway, rock slope destabilization is a widespread phenomenon and a major source of risk for the population and infrastructure. However, the lack of precise understanding knowledge of the permafrost distribution in steep slopes hinders the assessment of its role in these destabilizations. This study proposes the first nation-wide permafrost probability map for the steep slopes of Norway (CryoWall map). ~~It is~~ based on a multiple linear regression model fitted with multi-annual rock surface temperature (RST) measurements, collected at 25 rock ~~wall~~ slope sites, spread across a latitudinal transect (59-69°N) over mainland Norway. The CryoWall map suggests that discontinuous permafrost widely occurs above 1300-1400 and 1600-1700 m a.s.l. in the north and south rock faces ~~slopes~~ of southern Norway (59°N), respectively. This lower altitudinal limit decreases in northern Norway (70°N) by about 500±50 m, with more pronounced decrease for south faces, ~~in-reason~~ as a result of the insolation patterns largely driven by midnight sun in summer and polar night in winter. Similarly, the mean annual RST differences between north and south faces of similar elevation range around 1.5°C in northern Norway and 3.5°C in southern Norway. The CryoWall map is evaluated against direct ice observations in steep slopes and discussed in the context of former permafrost studies in various types of terrains in Norway. We show that permafrost can occur at much lower elevations in steep rock slopes than in other terrains, especially in north faces. We demonstrate that the CryoWall map is a valuable basis for further investigations related to permafrost in steep slopes in both practical concerns and fundamental science.

1 Introduction

Permafrost affecting steep bedrock slopes has been increasingly studied since the early 2000s in conjunction with both the high frequency of rock-fall activity during hot summers (e.g.- Gruber et al., 2004a; Fischer et al., 2006; Allen et al., 2009; Ravelin et al., 2017), and the occurrence of high-magnitude rock-ice avalanches (e.g. Haerberli et al., 2004; Sosio et al., 2008; Huggel et al., 2012; Deline et al., 2015). These increasing rock slope failures bear both fundamental and societal concerns. They are essential events of periglacial and paraglacial mass wasting processes (McColl, 2012) and of sediment transport (Korup, 2009). They are therefore important processes of landscape development, but are also important sources of hazard, threatening infrastructures, activities and individuals either by direct hit or by potential secondary effects, such as displacement waves and catastrophic flooding through debris flows (e.g. Huggel et al., 2005; Romstad et al., 2009; Hermanns et al., 2013).

Investigations of the mechanical behaviour of frozen bedrock have demonstrated that permafrost dynamics

Permafrost processes affect rock-wall stability as much on short as on long time scales (days to millennia). By modifying the bedrock and ice mechanical properties (Krautblatter et al., 2013), bedrock warming modifies the fracture toughness of rock bridges at depth > 20 m, preparing slow deformation and high-magnitude failures, while warming of ice-filled fracture joints at shallower depth is responsible for fast deformation and smaller magnitude rock detachments (Krautblatter et al., 2013). Recently, the study of Mamot et al. (2018) have established a new failure criterion to quantitatively predict the lowering of shear resistance of ice joints in bedrock fractures resulting of both, warming and unloading due to preliminary failures. It explains that the shear strength of an ice-filled fracture decreases by 64 to 78% when the shallow 4-15 m of the bedrock warm from -10 to -0.5°C. Permafrost aggradation provokes ice segregation processes, which prepare high-magnitude slope failure by favouring fracture propagation at depth (Matsuoka and Murton, 2008). Other studies have rather focused on the effect of Permafrost degradation can critically modify the shear strength of ice-filled fractures, with the most critical conditions being between -2 and 0°C (Davies et al., 2001). Water circulation resulting of active layer thaw and permafrost degradation, and showed that it ng in ice-free or partly ice-filled fractures could also accelerate the melting of ice-filled fractures in joints (Hasler et al., 2011a), while hydrostatic pressures caused by hydraulic permeability of ice-sealed fractures also addings to slope destabilization due to enhanced water pressures (Fischer et al., 2010; Krautblatter et al., 2013). The mechanical behaviour of frozen bedrock is therefore closely linked to its temperature range and water phase changes. For this reason, assessment of permafrost distribution and evolution in steep rock slope has been an important focus tackled by geomorphologists within the past fifteen years.

Since the Rock-slope failures jeopardize infrastructures, activities and individuals in the either by direct hit or by potential secondary effects, such as displacement waves and catastrophic flooding through debris flows (e.g. Huggel et al., 2005; Romstad et al., 2009; Hermanns et al., 2013).

Finally, rock fall and rock avalanches are essential agents of periglacial and paraglacial mass-wasting processes (Ballantyne, 2002), and mass-wasting and sediment transport sources in general (Korup, 2009). The role of the thermal regime as a significant driver for landscape-forming processes has been emphasized recently (Berthling and Etzelmüller, 2011), and developed in modelling approaches to understand landscaping processes (e.g. Hales

and Roering, 2007; Egholm et al., 2015). It is evident that the understanding of thermal regime within mountain slopes, and its development during past and the future, has significant relevance for geomorphology. early 2000s, rock surface temperature (RST) sensors have been deployed in many mountain areas, especially in the European Alps (e.g. Gruber et al., 2004b; Magnin et al., 2015a; Kellerer-Pirklbauer, 2017), but also in the Southern Alps of New Zealand (Allen et al., 2009), in the highest mountain peaks of Norway (Hipp et al., 2014), and in British Columbia (Hasler et al., 2015). Analyses of the recorded RST have shown that the primary factors controlling permafrost distribution and changes are the incoming short-wave solar radiation (or sun-exposure) and the air temperature (or elevation). Based on these findings, energy balance models have been employed to estimate the spatial distribution of rock slope permafrost (Gruber et al., 2004b), and combined with heat conduction schemes to assess its spatial patterns and evolution in typical alpine topographies (Noetzli et al., 2007; Noetzli and Gruber, 2009). Later, the accumulation of multi-year RST data over various mountain ranges has allowed the calibration of simple statistical models explaining the mean annual RST (MARST) with potential incoming solar radiation (PISR) and mean annual air temperature (MAAT) used to map permafrost over large areas (e.g. Boeckli et al., 2012a; Hipp et al., 2014; Magnin et al., 2015b). Nevertheless, RST measurements have also hinted at a significant control of snow accumulation on surface ruggedness, which has been investigated by mean of physic-based models (e.g. Haberkorn et al., 2017; Magnin et al., 2017a). These numerical investigations have shown that the high spatial and temporal variability of snow deposits in such steep slopes, due to the interaction of various topoclimatic factors (slope angle, sun-exposure, wind transport, etc.), result in a highly variable and local thermal effect, either warming or cooling the rock surface. This effect is therefore hardly accounted for in statistical approaches, but can be qualitatively assessed to interpret permafrost distribution maps (Boeckli et al., 2012b). These maps are essential bases to implement physic-based models in order to address the temporal evolution of steep slope permafrost and its interactions with environmental variables in areas where no temperature measurements are available (e.g. Magnin et al., 2017b). Furthermore, permafrost maps allow to link the observed rock wall destabilizations with permafrost conditions (e.g. Ravelin et al., 2017), and are therefore a key-step towards assessment of rock slope failures patterns and processes.

In Norway, the glacially shaped deep valleys and fjords are prone to mass-wasting processes. Rock-slope failures from the oversteepened slopes and potential secondary effects, such as displacement waves, represent one of the ~~most deadly~~deadliest natural hazards in the country (Furseth, 2006; Hermanns et al., 2012). Over the last 500 years, approximately 800 events and 500 fatalities have been recorded ~~throughout the country~~in Norway, among which three displacement waves, triggered by major rock-slope failures, caused the loss of 175 lives during the 20th century (Furseth, 2006; Hermanns et al., 2013; 2014). At present, more than 253 unstable rock slopes have been mapped systematically, and are partly monitored periodically by the ~~Norwegian geological survey~~Geological Survey of Norway (Oppikofer et al., 2015). At one of seven rock-slope instabilities, that are continuously monitored because of the potentially severe consequences in case of failure, ~~the role of permafrost was investigated with~~ direct observations ~~which~~ allowed for a detailed assessment about ~~the-its role of permafrost~~in local rock-wall dynamics (Blikra and Christiansen, 2014). Many of these unstable slopes are ~~most likely~~possibly located at or above the lower boundary of altitudinal permafrost. ~~Thus, a systematic investigation of steep rock slopes permafrost at the national scale is required in order to~~ (Hilger et al., 2018). However, the

lack of knowledge about its precise distribution in steep slopes precludes a systematic assessment of its role in the conditioning of rock slope failures.

Permafrost has been investigated in many different types of terrain at the site scale or national scale in Norway and Scandinavia. Monitoring networks have been deployed in gentle mountain slopes and mires of northern and southern Norway in the frame of national and international research programs (e.g. Ødegård et al., 1992; Harris et al., 2001; Christiansen et al., 2010; Isaksen et al., 2011; Farbrøt et al., 2011). Numerical models have been used to assess the permafrost distribution at the national and Scandinavian scales (Westermann et al., 2013; Gislås et al., 2013; 2016; 2017). The study of permafrost in steep slopes in Norway has recently started with direct measurements of rock surface temperature (RST) in the high-elevated alpine areas of Jotunheimen and Hurrungane (Hipp et al., 2014). Myhra et al. (2017) have simulated the permafrost evolution since the end of the Little Ice Age (1880) to present, for steep mountain sites spread over a latitudinal transect over Norway. At the national scale, a first-order estimation of the permafrost distribution in steep slopes has been proposed by Steiger et al., (2016), based on a straight-forward empirical relationship between air and rock-wall surface temperatures. Finally, Frauenfelder et al. (2018) studied ground thermal and geomechanical conditions in a permafrost-affected rockslide site in Troms (northern Norway). It is likely that changing rock and ice-temperatures, due to general warming and in response to the extreme warm previous year, have played an important role in this detachment.

Knowing the current distribution of permafrost is not only a prerequisite to assess its past, present and future variability, as well as but also to provide key-knowledge and tools to land-use-planners and earth scientists/geomorphologists. Thus, the lack of precise knowledge regarding the nation-wide distribution of steep rock slope permafrost is a major gap for both fundamental research and practical concerns in Norway. Therefore, we have monitored the RST at 25 measurement points, covering various aspects and elevations across a latitudinal transect of Norway. With the collected data we to (i) characterize the thermal regime in steep-rock slopes, (ii) calibrate a statistical model of RST and (iii) map permafrost probability for steep-rock slopes at the national scale. In this paper, we present (i) the measurement settings and strategy, (ii) the approaches for statistical modelling and permafrost probability mapping, and (iii) the permafrost distribution in steep slopes at the national scale and for local areas of interest.

2 Study area

The Norwegian mainland has a land area of c. 350000 km², and is dominated by the Scandinavian mountain chain of the Scandes, stretching between 57 – 71 °N through Norway and Sweden over a distance of more than 2000 km. Scandinavia forms a tilted margin, with highest elevations (culminating at 2469 m a.s.l.) found towards the western coast, and decreasing towards the east and the Bothnian Sea. The area has undergone multiple glaciations during the Pleistocene, with the largest glaciations covering northern Europe completely several times during the last c. 1 Mio. yrs (e.g. Kleman et al., 2008). Most of the land area in Norway is dominated by gentle relief landscape (Etzel Müller et al., 2007), probably preserved under cold-based ice conditions during the major glaciations (e.g. Kleman et al., 1999). Steep slopes and rock walls are mainly associated to four types of settings (e.g. Steiger et al., 2016): (i) steep valley sides associated to large U-shaped

valleys which drained the ice sheets during the glaciations, (ii) rock walls formed by local glaciations, mostly located along the western coast of the country and within the highest mountain regions of central southern Norway, (iii) rock walls associated to overthrust nappes, ~~such as in Hallingskarvet~~, and (iv) rock walls associated to steep river incisions, ~~such as Alta canyon (Čávža in Sami) in Finnmark~~. High-relief areas of Norway have experienced a high rock-slope failure activity throughout the late Pleistocene and Holocene, with a peak shortly after deglaciation (Böhme et al. 2015, Hermanns et al. 2017). The result is a high density of rock-slope failure deposits ~~and colluvial slopes~~ (e.g. Hilger et al., 2018), both in western and northern Norway. ~~The occurrence of actively deforming rock slope instabilities demonstrates the ongoing paraglacial landscape response towards natural stability equilibrium.~~

In general, the lower limit of mountain permafrost in Scandinavia decreases from the western coast towards eastern Norway and north-western Sweden, while the glaciation limit increases from west to east (e.g. King, 1983, 1986; Etzelmüller et al., 2003a). These gradients follow the climatic setting, with the maritime climate along the western coast (moist and high snow cover) gradually changing towards a more continental climate in the eastern parts of Norway (dry and less snow cover). In southern Norway, permafrost is mostly associated with bedrock in mountain settings, with coarse ground moraines and regolith (Farbrot et al., 2013; Gislås et al., 2013; 2017; Christiansen et al., 2010; Westermann et al., 2013), with the lower limit of discontinuous permafrost decreasing from c. 1600 m a.s.l. in the west to c. 1200 m a.s.l. in the east (Etzelmüller et al., 2003a). In northern Norway, on the other hand, the permafrost limit decreases from 800-900 m a.s.l. in the western mountains of Troms county, to 200-300 m a.s.l. in more continental areas, where it is often found in depressions characterized by peat plateaus (Borge et al., 2017).

The ongoing thawing and degradation of permafrost since the Little Ice Age (LIA) is likely to continue within the 21st century, with the lower altitudinal limit projected to rise up to 1800-1900 m a.s.l. in southern Norway (Hipp et al., 2012). Projections at the national scale based on an equilibrium model suggest that stable permafrost will be confined to 0.2% of mainland Norway by the end of the 21st century while it occupies about 6-6.5% of the ground at present, and was extending over 14% of the ground at the end of the LIA (Gislås et al., 2013). At present, we can expect considerable areas in Norway with thawing and degrading permafrost, which at greater depths is likely also a transient response to post-LIA warming.

3 Methods

3.1 Rock surface temperature monitoring

During the summers of 2015 to 2017, twenty-one temperature loggers (Geoprecision, M-Log5W-ROCK) were installed in eight mountain areas to record RST ~~at a depth of 10 cm~~ with a 2-h interval (Fig. 1). ~~Together with the remaining four out of five temperature loggers installed in 2010 in Jotunheimen (Hipp et al., 2014), a network of twenty-five temperature loggers was available for this study. In order to represent a wide range of climate settings, they were distributed between 60.33° N and 69.46°N, from 230 to 2320 m a.s.l., and in various aspects (Table 1, Fig. 2, Fig. S1).~~

The installation procedure followed the approach described by Gruber et al. (2004a2004b) by placing sensors at a depth of 10 cm and well above flat ground to avoid rapidly fluctuating surface temperature prone to erroneous measurements and ensure snow-free conditions. This Thick snow accumulation over the logger would make the recorded RST unsuitable for statistical modelling since it is unreliable to account for snow in such approaches because its thermal effect is not linear and depends on a variety of parameters that are highly fluctuating in space and time in high-elevated and high-relief environments such as the snow thickness, duration and time period of the accumulation, the sun-exposure of the affected rock face, and the snow pack thermal properties (Haberkorn et al., 2015; 2017; Magnin et al., 2015a; 2017a). Boeckli et al. (2012a) have shown that a precipitation or a “seasonal” variable have no statistical significance in their “rock model”, and confirmed that accounting for snow in statistical approach of steep rock slope permafrost is so far, hardly feasible. This is due to the high variability of snow in space and time in steep slopes, resulting from the interactions between topographical and topoclimatic factors controlling the snow thickness, distribution and thermal properties, and that produce highly fluctuating thermal effects (Haberkorn et al., 2015; 2017; Magnin et al., 2015a; 2017a).

Together with the remaining four out of five temperature loggers installed in 2010 in Jotunheimen (Hipp et al., 2014), a network of twenty-five temperature loggers was available for this study. In order to represent a wide range of climate settings, they were distributed between 60.33° N and 69.46°N, 230 to 2320 m a.s.l., and in various aspects (Table 1, Fig. 2). Specific attention was paid to the topographical settings, to make sure that the loggers are not covered by snow during winter. This would make the recorded RST unsuitable for statistical modelling since it is unreliable to account for snow in such approaches. This is due to the high variability of snow in space and time in steep slopes, resulting from the interactions between topographical and topoclimatic factors controlling the snow thickness, distribution and thermal properties, and that produce highly fluctuating thermal effects (Haberkorn et al., 2015; 2017; Magnin et al., 2015a; 2017a).

3.2 Linear regression modelling and permafrost probability calculation

The mean annual rock surface temperature (MARST) is mainly governed by incoming short-wave solar radiation (PISR) and mean annual air temperature (MAAT) which makes its estimation possible by mean of multiple linear regression model (sect.1; RST in steep slopes can be modelled by calculating the energy balance at the site (Gruber et al., 2004b), but for a regional survey with high spatial resolution, a statistical approach is better suited. Boeckli et al., 2012a; Hipp et al., 2014; Magnin et al., 2015b) such as:

$$Y = \alpha + \sum_{i=1}^k \beta_i X_i + \varepsilon \quad (1)$$

in which Y is the response variable (the MARST), α is the intercept term, $\beta_i X_i$ are the model's k explanatory variables (PISR and MAAT) and their respective coefficients to be calculated, and ε is a normally distributed residual error term which the mean is equal to 0 and the variance $\sigma^2 > 0$. From earlier investigations, it is widely accepted that RST is mainly related to incoming short-wave solar radiation and air temperature (Gruber et al., 2004b, Hipp et al., 2014). These two parameters are easily obtained over larger regions and with sufficient

- Mis en forme : Police :10 pt
- Mis en forme : Police :10 pt
- Mis en forme : Police :10 pt
- Mis en forme : Police :10 pt
- Mis en forme : Police :10 pt
- Mis en forme : Police :10 pt
- Mis en forme : Police :10 pt
- Mis en forme : Police :Times New Roman
- Mis en forme : Police :+Titres (Cambria)
- Mis en forme : Police :(Par défaut) Times New Roman, 10 pt
- Mis en forme : Police :(Par défaut) Times New Roman, 10 pt
- Mis en forme : Police :10 pt
- Mis en forme : Police :10 pt
- Mis en forme : Police :10 pt
- Mis en forme : Police :(Par défaut) Times New Roman, 10 pt
- Mis en forme : Police :10 pt
- Mis en forme : Espace Avant : 0 pt, Après : 10 pt
- Mis en forme : Police :10 pt
- Mis en forme : Police :10 pt
- Mis en forme : Police :(Par défaut) Times New Roman, 10 pt
- Mis en forme : Police :(Par défaut) Times New Roman, 10 pt
- Mis en forme : Police :10 pt
- Mis en forme : Police :(Par défaut) Times New Roman, 10 pt
- Mis en forme : Police :(Par défaut) Times New Roman, 10 pt
- Mis en forme : Police :(Par défaut) Times New Roman, 10 pt
- Mis en forme : Police :(Par défaut) Times New Roman, 10 pt
- Mis en forme : Police :10 pt
- Mis en forme : Police :(Par défaut) Times New Roman, 10 pt

spatial resolution, and thus available for multiple linear regression modelling. In a similar statistical approach, Boeckli et al. (2012a) have tested the role of precipitation and its seasonality, which have shown no significance.

In this study, we therefore predict the ~~Mean Annual RST~~MARST ($MARST_{pred}$) for the steep slopes of Norway as follows:

$$MARST_{pred} = a + PISR \times b + MAAT \times c \quad (42)$$

where a is the $MARST_{pred}$ value when PISR and MAAT are equal to 0, PISR and MAAT are respectively the Potential Incoming Solar Radiation (PISR) and the Mean Annual Air Temperature (MAAT) at measured RST~~logger~~ positions, with their respective coefficients b and c to be calculated. We therefore use the measured RST over several years to calculate a sample of MARST, for which we then calculate the PISR and MAAT at their locations (see following section for preparation of these variables) to fit the regression displayed in Equation (2) and calculate a , b and c using R (R Core team, 2013).

The model performance is assessed by the R^2 , RMSE (Root Mean Square Error) and MAE (Mean Absolute Error), while the model residuals (measured $MARST - MARST_{pred}$) are used to evaluate the suitability of the data sample for the linear regression model. We further performed a repeated ten-fold cross validation approach, which allows testing the model performance by partitioning the data set into ten sub-samples from which nine are used to fit the model, while one is kept to test the model (Gareth et al., 2014). The process is then repeated for each sub-sample and the means of the calculated R^2 , RMSE and MAE for each run are then provided to evaluate model performance (~~RMSE~~ R^2_{cv} , $RMSE_{cv}$ and MAE_{cv}). Ten folds balance the possible bias or high variability associated to respectively low and high fold numbers.

Finally, the probability of permafrost occurrence $P(p)$ is expressed by the probability of $MARST_{pred}$ at a given location to be $\leq 0^\circ\text{C}$. To calculate p , $MARST_{pred}$ is first transformed into a normal variable ($MARST_{norm}$) of mean $\mu = 0$ and variance $\sigma^2 = 1$ with:

$$MARST_{norm} = (-MARST_{pred} - \mu_{pred}) / \sigma_{pred} \quad (23)$$

In which μ_{pred} and σ_{pred} are the mean and standard deviation of $MARST_{pred}$, respectively. The negative sign associated to $MARST_{pred}$ is necessary since we calculate the probability of $MARST_{pred}$ to be negative.

In the final step, p is calculated using a logistic approximation of the cumulative normal distribution developed by Bowling et al. (2009):

$$P(p) = \frac{1}{1 + e^{-(0.07056 \times MARST_{norm}^3 + 1.5976 \times MARST_{norm})}} \quad (34)$$

which ensures simplicity and accuracy in the permafrost probability calculation by guaranteeing a maximum absolute error in probability < 0.00014 according to the comparison of Eq. (3) with the cumulative standard normal distribution (Bowling et al., 2009).

3.3 Calculation of model variables and model parameters

In order to ensure the best possible fit between the measured MARST, calculated PISR and MAAT, suitability of the collected RST time series for linear modelling, a preliminary visual preliminary data control is performed to detect possible snow control which would decorrelate the surface temperature from the air temperature and incoming solar radiation. To do so, Ddaily means are computed from RST hourly records and plotted against local air temperature (AT) measurements (Fig. 3). Smoothing of the temperature curves and disconnection with AT oscillations are identified/hunted, since they indicate thick snow accumulation (Hanson and Hoelzle, 2004) which considerably influences the RST (Magnin et al., 2015a; Haberkorn et al., 2015; 2017). For all our RST time series, we notice that Ddaily RST data usually follows AT oscillations throughout the year (Fig. 3). In summer, the sensors, which are most exposed to solar radiation record higher RST than sensors located in shaded area, and higher RST than air temperature become warmer than both the air and the more shaded sensors. No obvious smoothing of the daily RST is found in the presented time series, making them all suitable for statistical modelling.

After this visual check, daily RST data are aggregated to mean annual values (MARST). For the eight loggers at Mannen, in Jotunheimen and in Alta, we retrieve the data before achieving a full last year of measurements. Therefore a few days are missing to allow calculating MARST over complete years and we filled the the records were interrupted by missing data. In order to calculate the MARST for the incomplete record the data gaps/missing data for the last few days are filled by fitting a linear regression with local AT measurements (daily averages). For this, AT time series showing the best correlation with RST time series were chosen (Table 2, Fig. S1). The RST data processing provides 85 MARST multi-year measurement points to fit the regression model.

MAAT for the measurement period is calculated for each MARST point, using local meteorological records at different elevations, from which a lapse rate is calculated. AT data were retrieved from the eKlima portal (http://sharki.oslo.dnmi.no/portal/page?_pageid=73,39035,73_39049&_dad=portal&_schema=PORTAL) from the Norwegian meteorological institute. Similarly to the RST reconstruction, weather stations are chosen based on the best correlation between daily AT and RST records. To derive the most accurate MAAT during-at location of the RST measurement-period/loggers, we calculate the lapse rate at a daily time step between relatively low- and relatively high-lying weather stations. When AT records are incomplete, an average lapse rate is calculated for the period of the gap (two months overlap on each side of the gap) and for each of the recorded years. This yields a standard lapse rate value for the period of the gap, taking into account that lapse rate values can vary significantly throughout seasons. The meteorological data used to reconstruct MAAT at each of the MARST locations are presented in Table 3.

The PISR is then calculated for each MARST point at an hourly resolution over one year and considering a transmissivity of 100% (no atmosphere) using the Spatial Analyst tools of ArcGIS (© ESRI, Redlands, CA, USA). PISR is highly sensitive to topographical settings (sun-exposure, slope and viewshed), and thus highly dependent on the quality and coverage of the DEM. For the Mannen, Narvik, Flåm, Loen and one of the Kåfjord

(Gammanjinni) sites, 1 m resolution DEMs were available (Norge digital), while a 10 m resolution DEM (© Statens Kartverk, Norway) is available for entire Norway. The 1 m resolution DEMs only cover the relevant summits, meaning that and relief shading effects from the surrounding peaks is neglected in the PISR calculation. We therefore conducted Aa sensitivity test of the PISR to relief shading based on the 10 m resolution DEM, and tested the effect of DEM resolution on the calculated PISR to choose which DEM to use for the final PISR calculation at logger locations. The test indicates that the relief shading effects are marginal on the summits, with maximal differences of 50 Wm^{-2} , while the effect of the resolution is crucial, especially close to the summits and ridges (see Fig. S2). This is due to the sharp topography which is hardly represented in medium-resolution DEM and can lead to differences ranging above 100 Wm^{-2} . We chose the PISR values to attribute to each MARST point by averaging 3 to 5 pixel values best matching the measured topographical parameters (slope angle, aspect and elevation) considering both DEM resolutions (1 m and 10 m), regardless of the DEM resolution since the slope angle and sun-exposure have a primary role compared to the relief shading effect. Results of the sensitivity analysis are provided in the Supplement together with the MARST, MAAT and PISR data used to fit the multiple linear regression model (Fig. S4S2, Tab. S1).

3.4 Permafrost mapping

MAAT and PISR are first mapped over the entire country based on the 10 m resolution DEM. The PISR is calculated using the same parameters as for the model explanatory variable: hourly time step and 100% transmissivity. The MAAT is mapped using the SeNorge2 dataset, which is interpolated from *in-situ* temperature observations over grid point elevations at 1 km resolution (Lussana et al., 2017), and daily AT grids available from 1957. For the downscaling to a 10 m resolution, we first averaged daily AT data of the normal period 1981-2010 to generate a 1 km resolution MAAT raster. Then, for each 1 km grid cell, an average lapse rate is calculated over a radius of 25 km (Fig 54). This regional lapse rate is then used to interpolate 1km MAAT grid to a 10 m resolution. The 25 km radius ensures a precision at the regional scale, representing the relatively high lapse rate of the maritime coasts and the relatively low lapse rates in the more continental areas, while smoothing local patterns and possible artefacts.

MARST_{pred} and permafrost probability are then mapped by implementing Eq. (42) and (34) in a raster calculator. Since the model is only valuable for steep slopes with restricted snow and debris covers, the map is only produced for slopes $> 40^\circ$, which is a conservative threshold above which a 10 m resolution DEM is expected to display steep slopes. Indeed, DEMs tend to underestimate slope values and taking a higher threshold value would exclude a large part of possible steep slopes. This however entails that slopes with possible snow deposit are considered in the mapping step. Nevertheless, the interpretation provided in the following section allow to interpret permafrost probability according to the rock face characteristics (slope angle, ruggedness and possible snow accumulations).

3.5 Permafrost classes and interpretation keys

The permafrost probability is calculated as a continuous variable ranging from 0 to 1 which is then classified into four permafrost classes according to the international permafrost classification standards (Brown et al., 1997):

- continuous permafrost for $p \geq 0.9$
- discontinuous permafrost- for $0.5 \leq p < 0.9$
- sporadic permafrost for $0.1 \leq p < 0.5$
- isolated permafrost ~~is-for~~ $p < 0.1$

Similarly to the Alpine-wide Permafrost Map covering the European Alps and its index interpretation keys (Boeckli et al., 2012b), the here proposed permafrost classes are interpreted against local bedrock ~~settings~~ favourability to snow accumulation (Fig. 5) and possible cooling effect of dense fracturing allowing air ventilation (Hasler et al., 2011b). Indeed, Generally fractured, mid-steep and rugged bedrock surfaces of steep bedrock slopes are generally characterized by colder conditions than vertical, unfractured and smooth bedrock surfaces because they allow snow accumulation, eventually debris accumulation and air ventilation in fractures, which all have an overall cooling effect (Hasler et al., 2011b; Magnin et al., 2015a; 2017a; Haberkorn et al., 2015). Nevertheless, snow cover can in some rare cases (thick accumulation in shaded rock faces) rather warm the rock surface compared to snow free conditions due to thermal insulation (Magnin et al., 2015a; Haberkorn et al., 2017). Finally, the transient effects of past colder conditions have to be addressed also in the interpretation of the permafrost probability map. This is the result of the effect of sparse snow deposits preventing from heating of direct solar radiation and the effect of air ventilation in fractures, which acts as a shortcut between the cold atmosphere and the subsurface (Hasler et al., 2011b; Magnin et al., 2015a; 2017a; Haberkorn et al., 2015). Therefore, the specific effects of snow accumulation, non-conductive heat transfers in bedrock clefts and transient effects from past climate that are not accounted for in our statistical approach have to be considered when interpreting the permafrost map for specific sites.

~~C(Fig. 5).~~ Continuous permafrost thus suggests its existence in all conditions, regardless of the bedrock conditions local settings. Discontinuous permafrost, the lower boundary of which corresponds to $MARST_{pred} = 0^{\circ}C$, suggests that it exists in most of the rock faces, except those ~~that that~~ are (sub-)vertical and compact and substantially exposed to sun-beams (mostly all aspects except North), or eventually north faces with thick snow cover. ~~Generally fractured and rugged surfaces of steep bedrock slopes are characterized by colder conditions than unfractured and smooth bedrock surfaces. This is the result of the effect of sparse snow deposits preventing from heating of direct solar radiation and the effect of air ventilation in fractures, which acts as a shortcut between the cold atmosphere and the subsurface (Hasler et al., 2011b; Magnin et al., 2015a; 2017a; Haberkorn et al., 2015).~~ Sporadic permafrost suggests that the MARST is most likely positive, but that permafrost can exists at depth because of permafrost exists only if the local settings are very favourable conditions, meaning that the slope surface is substantially rugged and therefore more significantly fractured, covered by heterogeneous and

non-insulating snow and possible debris retention, or because of transient effects. Finally, isolated permafrost refers to isolated and perennial ice bodies found in open bedrock fractures at relatively low elevation.

4 Results

4.1 Model variables and summary statistics

The lowest MARST registered over the measurement period (Tab. 4) is found at Juv_4S (-4.9°C), the second highest measurement point, in 2012-2013, while the highest MARST (3.5°C) is registered at Fla_S in 2017-2018, which is the most sun-exposed sensor installed at the lowest latitude. The minimum and maximum MAAT values, respectively -5.9 and 0.4°C, are found at the highest and lowest measurement points, respectively: i.e. Juv_Eh5 in 2010-2011 and Alt_S in 2016-2017. The lowest PISR value (10 W.m²) is at Fla_N, the most shaded sensor of the lowest latitude, and the highest one (295 W.m²) is at Adj_S, a high-elevated and south-exposed logger in northern Norway (Fig. 5).

At eleven loggers, the measurements directly suggest permafrost occurrence (negative MARST every year). Permafrost-free conditions (positive MARST every year) are suggested at nine loggers with recorded MARST consistently > 1°C, and possible permafrost, with MARST oscillating between -1 and 1.5°C is found at 5 loggers (see Tab. S1). The presence of permafrost is nevertheless not excluded where positive MARSTs are recorded, because of the transient effect at depth from former colder periods (Noetzli and Gruber, 2009; Myhra et al., 2017), and a possible temperature offset (i.e. temperature difference between the surface and depth) resulting from the fracturing and snow deposits (Hasler et al., 2011b).

The MARST difference between north-exposed and south-exposed faces is around 3.5°C in southern Norway (e.g. 3.5°C at Fla_S and 0.2°C at Fla_N in 2017-2018), while it is around 1.5°C in northern Norway (e.g. 0.2°C at Adj_S and -1.4°C at Adj_N in 2015-2016). This difference between northern and southern Norway coincides with higher PISR values at north-exposed slopes of northern Norway, with for example 100 W.m⁻² more at Adj_N or Gam_N than at Fla_N or Man_N.

Table 5 summarizes the statistics of the regression model. For most of the measurement points, the MARST is generally higher than the MAAT (Fig. 6a) and the difference between MARST and MAAT (surface offset) increases with increasing PISR (Fig. 6b), confirming previous studies of steep bedrock thermal characteristics (Boeckli et al., 2012a; Magnin et al., 2015a). The surface offset ranges from 0 to 4°C, the highest values being found at the most sun-exposed sites, mostly located in high-elevated south-, east- and west-exposed faces whatever the latitude (Fig. 6b, Tab. S1). In some rare cases, the MARST is slightly lower than the MAAT (Fig. 6a), which indicates possible local factors locally cooling the most shaded rock faces (wind or ice accretion for example). An increase of 100 W.m⁻² induces an increase of about 1°C in MARST and is equivalent to an increase of 1°C in MAAT. The adjusted R², RMSE and MAE demonstrate the good fit of the model, which is

corroborated by the consistency of these values with those of the R^2_{cv} , $RMSE_{cv}$ and MAE_{cv} (Tab. 5) ~~from our cross-validation procedure~~. The model residuals confirm that the data sample is well suited for the chosen statistical approach (Fig. 7): they are randomly distributed around 0°C, and no noticeable outlier is detected.

4.2 Permafrost distribution in steep slopes

Steep slopes represent almost 2% of the surface area of mainland Norway, constituting about 7300 km² between sea level and 2460 m a.s.l. (surface area covered by slopes $> 40^\circ$ on the 10 m resolution DEM). The rock wall surface area is unequally distributed across latitudes with almost 20% lying between 61 and 62°N (Fig. 8a), where the highest peaks of Norway are ~~located~~ (Fig. 8b). West-facing slopes are generally predominant (30%), while south-exposed faces are less frequent (20%), and north and east facing-slopes each represent a quarter of the steep slope surface area. However, this ~~global-national~~ pattern is not constant across latitudes, with for example, predominantly north-facing slopes between 65 and 67°N (Fig. 8a).

Continuous permafrost occupies about 2% of the rock wall surface area, discontinuous permafrost about 9% and sporadic permafrost about 20%, meaning that 31% of the rock wall surface area features a permafrost probability ≥ 0.1 and 11% a probability ≥ 0.5 .

In Figure 9 we display the distribution of the lowest occurrence of each permafrost class (*i.e.* the distribution of the occurrences of probability 0.1, 0.5, and 0.9) according to elevation and latitude. We refer to these lowest occurrences as the “lower altitudinal limit” (LAL) of each permafrost class. In the southernmost part of Norway (58°N), sparse occurrences of sporadic permafrost are found as low as 830 m a.s.l. in all aspects, except south (Fig. 9). Discontinuous permafrost occurs from 59°N ~~with the lowermost observations of the lower altitudinal limit (LAL) as low as~~ 1150 m a.s.l. in north faces, and 50% of the LAL observations above 1300-1400 m a.s.l.. At the same latitude, sparse occurrences of continuous permafrost are found from 1700 m a.s.l. in north and east faces. Continuous permafrost is more widespread at 61 and 62°N, in accordance with rock wall frequency and elevation. The 1st quartile of the observations of LAL of continuous permafrost is around 1500 m a.s.l. in north faces, 1700 m a.s.l. in east and west faces, and 1900 m in south faces. Little permafrost is found in the steep ~~bedrock~~ slopes between 63 and 65°N, concordant with rock-wall frequency and elevation, ~~and therefore result in a plateau-like pattern in the distribution of permafrost across latitude~~. From 67 to 69°N, continuous permafrost exists mostly above 1100 m a.s.l. in north faces, 1200 m a.s.l. in east and west faces, and 1400 m a.s.l. in south faces. The LAL for discontinuous permafrost decreases from 900 to 700 m a.s.l. in north faces, over 800-900 m a.s.l. for east and west faces, and down to 1000 m a.s.l. for south faces between 67 and 69°N. Sparse occurrences of discontinuous permafrost are found as low as 50 m a.s.l. in all aspects at 69 and 70°N. At 70°N, the ~~highest~~ permafrost probability ~~reaches a maximum value of is~~ 0.9, meaning that continuous permafrost is mostly absent, mainly because ~~the elevation of~~ rock walls rarely exceed 1000 m a.s.l..

The medians of observations of the LAL of each permafrost class decrease by about 500 ± 50 m from southern to northern Norway, decreasing by about 50 m with every degree northwards for north facing slopes, and ~~with by~~ 58 m for the south facing slopes. For example, the median of the observations of the LAL of discontinuous permafrost at 60°N is at 1210 m a.s.l. and 1580 m a.s.l. in the north and south faces respectively, and at 760 m a.s.l. and 1060 m a.s.l. at 69°N. In southern Norway, permafrost therefore exists 350 to 400 m lower in north faces compared to south faces, while it is ~~found only~~ 200 to 250 m lower in northern Norway. These decreases in the LAL of permafrost classes according to latitude and aspect do not appear linear (Fig. 9) because the rock-wall distribution significantly controls this relationship (Fig. 8). ~~However, there is a high correlation between the distribution of the 0°C isotherm (lower limit of discontinuous permafrost) and latitude (Fig. 10). The lower limit of permafrost decreases by about 60 m every degree northwards for north faces and almost 70 m for south facing slopes.~~

The number of ~~rock slope~~ permafrost observations decreases with continentality (Fig. 10) as most of the rock walls are found ~~in the Caledonides~~ close to the coast and in the ~~interior-western~~ mountain massifs of southern Norway such as Jotunheimen, Rondane or Dovrefjell (Fig. 11). ~~In relation to continentality, the~~ This decrease in observations makes a statistical analysis of permafrost distribution ~~according to continentality~~ poorly relevant. Nevertheless, we note that the lowermost occurrences of discontinuous permafrost in north faces of southern Norway are found at the furthest distance from the sea, in Sølen, Sennsjøkampen, and the border with Sweden in the Nesjøen area (Fig. 10 and 11). In northern Norway, the lowermost occurrences of discontinuous permafrost are not found near the coast, but further inland (about 25 to 50 km away from the sea, Fig. 11). At such distance, low-elevated rock walls (< 200 m a.s.l.) are mostly found in river canyons, such as at the Alta, Reisa or Tana rivers (Fig. 11). It is also noteworthy that in ~~the~~ general, the dominant areas of permafrost rock walls are located west of the main distribution of permafrost in Norway according to *e.g.* Gissnås et al. (2017).

5 Discussion

5.1 Model evaluation

To evaluate the permafrost probability model, we compare the permafrost probability map for the steep slopes of Norway, named “CryoWall map” in the following, to the rare permafrost evidences and studies in steep slopes of Norway. Unlike gentle slope permafrost, ~~on~~ which ~~produces~~ typical landforms, such as rock glaciers or palsas and peat plateaus ~~occur~~, permafrost in steep slopes only becomes evident by ice in rock fractures or failure scars. In northern Norway, Blikra and Christiansen (2014) observed sporadic permafrost in the fractures of the Jettan rock slide, extending from 400 to 800 m a.s.l., which is corroborated by the CryoWall map (Fig. 11 and 12a). About 45 km southwest of Jettan, ~~the detachment of~~ a 500,000 m³; ~~in June 2008~~, rock mass ~~detached-uncovered ice in the scar~~ from the ~~e~~East face of Polvartiden (1275 m a.s.l.) ~~in June 2008~~, ~~from an elevation of 600 m a.s.l.~~, ~~uncovering ice in the scar~~. Frauenfelder et al., (2018) simulated permafrost in the Polvartinden summit by mean of 2D numerical modelling tools based on several years of rock wall temperature information. These simulations estimated a lower limit of permafrost (0°C isotherm) at about 650 m, which is the top of the rock slope failure

and the lower limit of discontinuous permafrost ([also 0°C isotherm in our approach](#)) suggested by the CryoWall map (Fig. 12b).

In southern Norway, Etzelmüller et al. (2003b) report that ice was found during construction work in the 1950s at about 1500-1600 m in the bedrock of Gaustatoppen (1883 m a.s.l.), where the CryoWall map indicates discontinuous permafrost (Fig. 12c). Gaustatoppen is made of Precambrian quartzite, prone to macrogelivation and therefore to the producing of geometric blocks (Sellier, 1995). Combined with slopes rarely exceeding 55°, this results in a significant debris cover, favouring snow accumulation in winter and permafrost persistence, even with a relatively low probability value. Protruding rock outcrops also exists at Gaustatoppen, but they are generally highly fractured and covered by thin snow in winter, which makes them also favourable to permafrost persistence.

In relation to the study by Steiger et al. (2016), this approach is an improvement as (i) we calibrate our model with observations and therefore account for the important influence of topographic aspect, (ii) we use an updated and improved spatial interpolation method for [2-m-AT air temperature](#) that has been used to build the SeNorge2 dataset (Lussana et al. 2017), [and](#) (iii) we downscale AT using a regional lapse rate instead of using a standard and uniform one. The main pattern of steep-slope permafrost distribution is comparable, while locally deviations related to sun-exposure are substantial. For example, Steiger et al. (2016) suggested a lower limit of rock wall permafrost around 850 m a.s.l. in the Lyngen Alps, which is the limit of the third quartile of the observations of the LAL of discontinuous permafrost in north faces, and below the first quartile of these observations in the north faces (Fig. 15). Steiger et al. (2016) also found a lower limit of rock wall permafrost close to sea level in the Varanger Peninsula (70°N) while the CryoWall map suggests discontinuous permafrost above 100 m a.s.l. only (Fig. 15).

Comparison with results from Myhra et al. (2017) who modelled permafrost distribution and evolution since the LIA for four sites of Norway is limited because of the idealized test cases considered in this study, which do not account for local topographical characteristics and insolation. A comparative figure of the CryoWall map and Myhra et al. (2017) models is provided in the Supplement (Fig. [S2S3](#)).

5.2 Permafrost characteristics in the steep slopes of Norway compared to other areas

Permafrost affecting steep rock slopes has mostly been studied in rock walls of the European Alps (45-46°N), where the lower limit of the isotherm 0°C lies around 2800±300 m a.s.l. in north faces and 3800±300 m a.s.l. in south faces [of the Bernina and Mont Blanc massifs](#) (Gruber et al., 2004a; 2004b; Magnin et al., 2015b). This difference of about 1000 m elevation between north and south faces is directly imputed to the solar radiation control, which results in a MARST difference reaching 8°C between the north and south faces of a same elevation. In British Columbia (Canada), north faces are 4°C colder than south faces between 54°N and 59°N (Hasler et al., 2015). In the southern Alps of New Zealand, at 43°S, differences between north and south faces

reaching a maximum of 5°C were reported (Allen et al., 2009). Our study presents MARST measurements at higher latitudes, where smaller and decreasing north-south differences with latitude are observed. This is the result of less and more direct solar radiation in south and north-facing slopes, respectively, which is reinforced at higher latitude due to the polar night in winter and midnight sun during summer. This also explains the decreasing-greater difference of the between-the-LAL limit-of each permafrost class between south and north faces towards lower latitudes (Fig. 9, sect. 4.2), where the south faces receive more solar radiation, unbalancing the air temperature controls, while the north facing slopes receive less direct solar radiation and are more directly controlled by air temperature.

Despite the solar radiation control, which seems to be predominant in the rock slope RST-permafrost distribution patterns from local to continental scales, additional factors may also affect the RSTplay a role. The snow that accumulate in various thicknesses in steep slopes has been recognized as a significant factor affecting the RSTpermafrost conditions at the local scale in the European Alps, as it attenuates both, the winter cooling (Haberkorn et al., 2017) and the insolation heating in late winter and spring (Magnin et al., 2017b2017a). In Norway, snow and frost coating is common at (mainly due to atmospheric icing, i.e. high-elevation rock walls that are exposed to supercooled water in clouds and strong and if combined with strong wind. These heavy ice accretions and snow deposit on slope ruggedness it can produce heavy ice accretions) are common in some of the high-elevation areas, and can certainly provoke result in significant inter-annual variability of MARST in prevailing wind direction and preferential snow deposition (Frauenfelder et al. 2018). Furthermore, energy exchanges due to latent and sensible heat effects that are relatively more important in high-latitude and maritime settings than in more continental mountain areas possibly affect the RST-permafrost patterns. In the same way, cloudiness, that is generally more important in maritime settings, may also play an important role. This is evidenced by the relatively small north-south difference in the southern Alps of New Zealand (Allen et al., 2009) that are at a rather low latitude but famous for their high precipitation rates. This is confirmed by Sattler et al. (2016) who have attributed an unusually low permafrost limit in debris slope in the maritime areas of New Zealand to the frequent cloud cover in summer. Such effects are not easily detectable by mean of visual control or statistical analysis and point out the need for more physic-based investigations in order to better understand their respective influence on MARST patterns and permafrost distribution. However, the good fit of observations with the simple linear model indicates that such effects are only of minor relevance for Norway and do not strongly affect the overall permafrost distribution in steep slopes.

5.3 Permafrost characteristics in the steep slopes compared to other permafrost terrains in Norway

The distribution of permafrost has been estimated in various regions of southern and northern Norway by means of Bottom-bottom temperature of snow cover (BTS) measurements (Haeberli, 1973), rock glacier inventories, ground temperature monitoring, geophysical soundings and numerical models. Locations of the areas mentioned below are displayed on Figure 11.

In central southern Norway, the LAL of gentle slope permafrost decreases with continentality (Fig. 13), being at c. 1500 m a.s.l. in Jotunheimen (Isaksen et al., 2002; Farbrot et al., 2011), down to 1300 m a.s.l. in Dovrefjell ~~at sites with no snow cover~~ (Sollid et al., 2003; Isaksen et al., 2011; Westermann et al., 2013), and 1100 m a.s.l. in more eastern continental terrains in the Femunden region ~~with a thin snow cover~~ (Heggem et al., 2005; Westermann et al., 2013; Gislås et al., 2017). The CryoWall map confirms this general pattern across continentality (Fig. 10), but this decrease doesn't follow the same pattern in steep rock slopes as it is strongly dependent on sun-exposure (Fig. 13). ~~decreasing elevation of the lower limit of~~ For example, in permafrost across continentality (Fig. 10 and 13). However, the LAL of permafrost in gentle slopes of Jotunheimen, ~~the is close to the LAL lower limit of discontinuous permafrost in south-facing rock walls is at the same elevation as the lower limit of discontinuous permafrost observed in gentle slopes (Fig. S3a), while but 300-400 m higher than in the north-facing rock walls (Fig. 13).~~ At the local scale, the transition between continuous and discontinuous permafrost is similar in north-exposed rock walls than in gentle slopes, while discontinuous permafrost in south-exposed rock walls rather occurs in the continuous permafrost zone of for the surrounding gentle slopes (Fig. S3a). ~~In Dovrefjell further east, the LAL lower limit of discontinuous permafrost in gentle slopes rather corresponds to the lower LAL limit of discontinuous permafrost in north-exposed rock walls slopes (Fig. S3b), while it is about 200-300 m lower than in south-exposed rock walls. But at the local scale, the transition between continuous, discontinuous and sporadic permafrost coincides remarkably well to the map based on BTS measurement (Isaksen et al., 2002) produced by Etzelmüller (unpublished), even for south-exposed rock walls (Fig. S3b).~~ In the easternmost region eastern Norway, rock faces are rare and therefore evidences of permafrost distribution ~~ins~~ steep bedrock slopes are sparse and mostly limited to Sølen and Sennsjøkampen areas (see location on Fig. 11). However, ~~d~~Discontinuous permafrost is found as low as 960 m a.s.l. in the north face of Sennsjøkampen, and above 1290 m a.s.l. in south, east and west faces of Sølen (Fig. 13) ~~which).~~ This is generally higher than in surrounding slopes where permafrost generally occurs at much lower elevation (Heggem et al., 2005, Fig. S3c; Fig. S3e). Thus, there is an increasing discrepancy between permafrost distribution in steep and surrounding gentle slopes across continentality. The eastwards gradient in the lower limit of permafrost in gentle slopes is attributed to a decrease in the altitudinal limit of block fields and snow fall amounts (Farbrot et al., 2011), while in steep rock faces that are more coupled with the atmosphere, this is rather an effect of decreasing air temperature (Fig. 4). In the western maritime parts, thick snow cover prevents from intense cooling in winter, a general pattern already suggested by Gruber and Haeberli (2009). This insulating snow pack balances the cooling effect of block fields, while in the eastern continental part, this latter effect is predominant due to reduced snow cover. As a results, in western parts, the overall permafrost conditions in gentle slopes are more in accordance with air temperature (result of the counter effects of insulating snow cover and cooling block fields) and therefore with surrounding steep bedrock slopes. Conversely, in the eastern parts, ground temperature is much lower than the air, and therefore permafrost occurs at much lower elevation than in rock walls.

In northern Norway, the ~~lower limit~~LAL of discontinuous permafrost in gentle slopes and flat terrains lies around 800-900 m a.s.l. in the coastal mountains ~~of Troms county,~~ such as in the Lyngen Alps (Farbrot et al., 2013, Steiger et al 2016), and decreases to 300-500 m a.s.l. in the coastal areas and mires in the inner part of Finnmark such as the Varanger peninsula (Isaksen et al., 2008; Farbrot et al., 2013; Borge et al., 2017). ~~In the~~

interior part of the Varanger peninsula the lower limit of permafrost in gentle slopes and flat terrains is around 400–450 m a.s.l. (Isaksen et al., 2008). Observations in the coastal rock steep slopes of the Varanger peninsula (Fig. 13) show that permafrost can occur at lower elevations than in gentle slopes in coastal Finnmark. The only rock faces existing in the inner part of Finnmark are mostly the river canyons such as the Alta and Tana rivers, where discontinuous permafrost occurs between 100 and 600 m a.s.l. (Fig. 10 and 11), favoured by the high confinement and resulting low solar radiation input. The occurrence of permafrost may be underestimated in some places of continental areas due to local temperature inversion which are smoothed by the regional lapse rate calculation (e.g. Fig. 4).

5.4 Implications for landscape development and hazard assessment in Norway

The CryoWall map confirms most of the previous findings in terms of permafrost occurrence and distribution in steep rock slopes inferred from visible ice or numerical modelling experiments in Norway. It is therefore a reliable basis to assess permafrost distribution in the steep rock slopes rock wall permafrost in of Norway. The collected RST time series and CryoWall map may be used to model the permafrost evolution through time, using the predicted MARST map or the measured RST as upper boundary conditions for 1D or 2D simulation (Hipp et al., 2014; Magnin et al., 2017b, 2017a, 2017b). The permafrost models and the CryoWall map could then support investigations on large-scale rock slope deformations, slope hazards such as rock falls and the assessment of geomorphological processes. To illustrate some of the research problems our map can contribute to, we give some examples and analysis in the following.

Large-scale rock slope deformations in Norway – In the Norwegian mountains, numerous sites with large scale instabilities are identified through systematic mapping and surveillance during the last years (e.g. Hermanns et al., 2012; Bunkholt et al., 2013; Oppikofer et al., 2015). Seven sites comprise a high hazard level, justifying installation of an early warning system, two of which have been equipped with RST loggers in this study. We now used the CryoWall map to assess permafrost occurrence at “critical slopes” inventoried by the Geological Survey of Norway (Oppikofer et al., 2015, http://geo.ngu.no/kart/ustabilefjellparti_mobil/). The database comprises unstable slopes (postglacial deformation that could lead to catastrophic slope failures), deformed rock slopes that can produce rock falls, potential unstable slopes (that match the structural inventory for failure but have no signs of deformation), and morphological lineaments along steep slopes that are the result of erosional processes. Each critical slope is recorded as a point at about the middle of the slope. To extract permafrost probability at this point and overcome limitations related to the mismatch between the location of steep areas in the respective slopes and the location of the points, we created a buffer of 200 m around each point to ensure that the point surface areas cover most of the slope, including the steep parts. The maximum permafrost probability contained in the buffer area of each point was then extracted for 1339 registered critical slopes, and 11% of them are permafrost slopes (probability > 0.5). The distribution of these critical slopes is displayed in the Supplement (Fig. S4S5). This preliminary investigation points out the critical slopes that may deserve further investigations on the potential role of permafrost in their ongoing or possibly future destabilization, especially in the current context of climate change and permafrost degradation. As a further step, the hazard level could be statistically

linked to the permafrost probability following a similar approach as the one conducted by (Ravel et al., 2017) in the Mont Blanc massif.

Periglacial geomorphology—Rock glaciers and stable ice-cored moraines are the only landforms directly indicating permafrost presence in mountain regions (e.g. Berthling, 2011; Haeberli 2000; Etzelmüller and Hagen 2005). These landforms are normally associated to steep slopes, at least in the vicinity. We used a rock glacier/stable ice-cored moraine inventory for Norway (Lilleøren and Etzelmüller, 2011) and compared adjacent rock walls of active rock glaciers to our results. We found that most rock walls associated to active rock glaciers or to cirques where ice-cored moraines emerge, were classified as discontinuous to continuous permafrost, at least in their upper part (Fig. S5). This underpins the interest for studying the connection of permafrost rock walls and adjacent landforms which so far, to the author's knowledge, has not been directly addressed. Indeed, permafrost dynamics can influence material supply pattern to these landforms, as e.g. frost cracking varies greatly within and without permafrost environments (e.g. Hales and Roering, 2007).

Mis en forme : Police :Italique

Landscape development - It is evident that the understanding of thermal regime within mountain slopes, and its development during past and the future, has a geomorphological relevance (Berthling and Etzelmüller, 2011, Hales and Roering, 2007). Frost weathering and stabilisation/destabilisation of slopes over long time scales due to climate variability and glaciation cycles work in concert, and in certain temperature bands. For example, the frost cracking window, which is known as being between -8 and -3°C with positive gradient at depth (e.g. Hallet et al., 1991; Hales and Roering, 2007) defines a narrow temperature band, in which frost weathering processes are most effective, resulting in ice segregation and subsequent rock falls (e.g. Draebing et al., 2017). On the other hand, deep permafrost aggregation/aggradation/degradation weakens rock masses, with the possibility of larger-scale slope destabilisation on longer time scales (e.g. Krautblatter et al., 2013). Moreover, steep rock walls, often snow free or with little snow cover, can influence the thermal regime of adjacent areas due to lateral heat flux (Myhra et al., 2017), with the possibility to maintain large temperature gradients. All these processes influences material predication and erosion of mountain ranges and contribute to the periglacial realm being an important environment for weathering (Hales and Roering, 2007; Savi et al., 2015), valley formation (Büdel, 1981) and landscape planation ("periglacial buzzsaw") (e.g. Hales and Roering, 2009; Egholm et al., 2015).

Finally, the collected RST time series may be used for a detailed analysis of RST patterns over different environmental settings (climate, topography), and support the development of a possible and straightforward model of rock wall permafrost distribution at the continental scale (Sect. 5.2). This would require a systematic sampling of steep slopes to ensure their representativeness of idealized case directly coupled with the atmosphere and no specific topographical settings affecting their insolation, as well as further investigations on the atmospheric moisture and cloudiness controls.

6 Conclusions

From this study the following main conclusions can be drawn:

- Sporadic permafrost occupies about 20 % of the steep slope surface area in mainland Norway. It can be found as low as 830 m a.s.l. in north faces at 59°N and down to sea level in all aspect in northern Norway.
- Discontinuous permafrost occupies 9% of the rock wall surface area and can be found in southern Norway (from 59°N) mostly above 1300-1400 m a.s.l. in north faces and 1600-1700 in south faces. In northern Norway, it mainly occurs above 750 m a.s.l. in north faces and 1050 m a.s.l. in south faces.
- Continuous permafrost occupies 2% of the rock wall surface area between 59°N and 69°N, with substantial presence above 1500 m a.s.l. in north faces and 1900 m a.s.l. in south faces of southern Norway. In northern Norway, it is widespread above 1100 m a.s.l. in north faces, and 1400 m a.s.l. in south faces.
- The difference in mean annual rock surface temperature of north and south facing slopes at similar elevation is about 3.5°C in southern Norway and 1.5°C in northern Norway due to the effect of solar radiation in relation with the polar night/midnight sun effect at higher latitudes. The differences are substantially lower than in reported alpine areas of lower latitudes.
- The lower elevation limit of permafrost decreases by about 500±50 ~~for~~ between southern and northern Norway, with a more pronounced decrease for south-exposed slopes (-50_m for every degree northwards for north-exposed slopes against -58 m for the south-exposed ones).
- The lower elevation limit of permafrost also decreases across continentality, with occurrences of discontinuous permafrost about 200 m lower in eastern Norway than in the west coast of southern Norway, and below 200 m a.s.l. in the river canyons of northern Norway.
- Steep slope permafrost generally occurs lower than in gentle mountain slopes in north faces, but at higher elevation in south faces. This pattern is nevertheless more or less pronounced depending on the regions of Norway.

Data availability

The CryoWall map will be made available after publication via the NIRD research data archive: <https://archive.norstore.no/>

Authors contributions

FM led the preparation of the manuscript with guidance from BE, and input from SW, KI, PH and RH. The overall research project was conducted by BE with significant contributions from other authors. FM, BE, PH and RH participated in the installation of the rock temperature loggers and data collection. KI provided some meteorological data.

Acknowledgement

This study is part of the CryoWALL project (243784/CLE) funded by the Research Council of Norway (RCN). Additional funding, both directly or indirectly, was provided by the University of Oslo, the ~~Norwegian~~ Geological Survey ~~of Norway~~ and the Norwegian Water and Energy Directorate (NVE). ~~Part of the work by the~~

Norwegian Meteorological Institute was funded by the Research Council of Norway through the Climate Research Programme KLIMAFORSK (ACHILLES, project no. 235574). Bas Altena, Thorben Dunse, Justyna Czekirda, Jaroslav Obu, Ove Brynildsvold (all University of Oslo), Joel Fiddes (SLF, Switzerland), Amund Mundhjøld (Raubergstulen) and Solveig Winsvold (NVE) helped with either installing rock wall loggers or reading them out. C. Lussana (Meteorological Institute of Norway) guided the processing of the SeNorge2 dataset. We especially thank NVE, section for rock slide early warning ("Fjellskredovervaking") and its leader, Lars Harald Blikra, both in Stranda and in Kåfjord, Troms, for their enthusiastic support during field work and later discussions. We want to thank all mentioned individuals and institutions.

References

- Allen, S. K., Gruber, S. and Owens, I. F.: Exploring steep bedrock permafrost and its relationship with recent slope failures in the Southern Alps of New Zealand, *Permafrost and Periglacial Processes*, 20(4), 345–356, doi:10.1002/ppp.658, 2009.
- ~~Ballantyne, C. K.: Paraglacial geomorphology, *Quaternary Science Reviews*, 21(18), 1935–2017, doi:10.1016/S0277-3791(02)00005-7, 2002.~~
- Berthling, I., and Etzelmüller, B.: The concept of cryo-conditioning in landscape evolution. *Quaternary Research*, 75(2), 378–384, 2011.
- Blikra, L. H. and Christiansen, H. H.: A field-based model of permafrost-controlled rockslide deformation in northern Norway, *Geomorphology*, 208, 34–49, doi:10.1016/j.geomorph.2013.11.014, 2014.
- Boeckli, L., Brenning, A., Gruber, S. and Noetzli, J.: A statistical approach to modelling permafrost distribution in the European Alps or similar mountain ranges, *The Cryosphere*, 6(1), 125–140, doi:10.5194/tc-6-125-2012, 2012a.
- Boeckli, L., Brenning, A., Gruber, S. and Noetzli, J.: Permafrost distribution in the European Alps: calculation and evaluation of an index map and summary statistics, *The Cryosphere*, 6(4), 807–820, doi:10.5194/tc-6-807-2012, 2012b.
- Bohme, M., Oppikofer, T., Longva, O., Jaboyedoff, M., Hermanns, R. L., and Derron, M.-H.: Analyses of past and present rock slope instabilities in a fjord valley: Implications for hazard estimations, *Geomorphology*, 248: 464–474, 2015.
- Borge, A. F., Westermann, S., Solheim, I. and Etzelmüller, B.: Strong degradation of palsas and peat plateaus in northern Norway during the last 60 years, *The Cryosphere*, 11(1), 1–16, doi:https://doi.org/10.5194/tc-11-1-2017, 2017.
- ~~BowlingDavie, S. R., Khasawneh, M. T., Kaewkuekool, S. and Cho, B. R.: A logistic approximation to the cumulative normal distribution, *Journal of Industrial Engineering and Management*, 2(1), 114–127, doi:10.3926/jiem.v2n1.p114-127, 2009.~~
- Brown J, Ferrians OJ, Heginbottom JA, Melnikov ES. 1997. International Permafrost Association Circum-Arctic Map of Permafrost and Ground Ice Conditions, Map CP-45. US Geological Survey.
- Büdel, J. Klima-geomorphologie. 304 pp, Gebrüder Bornträger, Berlin, ISBN 978-3-443-01017-1, 1981.
- Bunkholt, H., Nordahl, B., Hermanns, R. L., Oppikofer, T., Fischer, L., Blikra, L. H., Anda, E., Dahle, H., and Sætre, S. Database of unstable rock slopes of Norway. In C Margottini, P Canuti and K Sassa (eds.), *Landslide science and practice*, 423–428, Springer, Berlin, Heidelberg, 2013.
- Christiansen, H. H., Etzelmüller, B., Isaksen, K., Juliussen, H., Farbrøt, H., Humlum, O., Johansson, M., Ingeman-Nielsen, T., Kristensen, L., Hjort, J., Holmlund, P., Sannel, A. B. K., Sigsgaard, C., Åkerman, J., Foged, N., Blikra, L. H., Pernosky, M. A. and Ødegård, R. S.: The thermal state of permafrost in the nordic area during the international polar year 2007–2009, [online] Available from: https://onlinelibrary.wiley.com/doi/10.1002/ppp.687 (Accessed 12 November 2018), 2010.

- Davies, M. C. R., Hamza, O. and Harris, C.: The effect of rise in mean annual temperature on the stability of rock slopes containing ice-filled discontinuities, *Permafrost and Periglacial Processes*, 12(1), 137–144, doi:10.1002/ppp.378, 2001.
- 5 Deline, P., Gruber, S., Delaloye, R., Fischer, L., Geertsema, M., Giardino, M., Hasler, A., Kirkbride, M., Krautblatter, M., Magnin, F., McColl, S., Ravel, L., and Schoeneich, P.: Ice Loss and Slope Stability in High-Mountain Regions In: *Snow and Ice-Related Hazards, Risks and Disasters* <http://dx.doi.org/10.1016/B978-0-12-394849-6.00015-9>, 2015.
- 10 Draebing, D., Krautblatter, M. and T. Hoffmann.: Thermo-cryogenic controls of fracture kinematics in permafrost rockwalls. *Geophysical Research Letters* 44(8): 3535–3544. <http://dx.doi.org/10.1002/2016GL072050>, 2017.
- Egholm, D. L., Andersen, J. L., Knudsen, M. F., Jansen, J. D., and Nielsen, S. B.: The periglacial engine of mountain erosion-Part 2: Modelling large-scale landscape evolution. *Earth Surface Dynamics*, 3(4), 2015.
- 15 Etzelmüller, B., Berthling, I., Sollid, J. L.: Aspects and concepts on the geomorphological significance of Holocene permafrost in southern Norway, *Geomorphology*, 52, 87–104. DOI:10.1016/S0169-555X(02)00250-7, 2003a.
- Etzelmüller, B., Berthling, I., and Ødegård, R.: 1-D-DC-resistivity depth soundings in high mountain areas of Southern Norway – a tool in permafrost investigations, *Z. Geomorph., Suppl. Bind*, 32, 19–36, 2003b.
- Etzelmüller, B., Romstad, B., and Fjellanger, J.: Automatic regional classification of topography in Norway: *Norwegian Journal of Geology - Norsk Geologisk Tidsskrift*, v. 87, p. 167–180, 2007.
- 20 Farbot, H., Hipp, T. F., Etzelmüller, B., Isaksen, K., Ødegård, R. S., Schuler, T. V. and Humlum, O.: Air and Ground Temperature Variations Observed along Elevation and Continentality Gradients in Southern Norway - Farbot - 2011 - Permafrost and Periglacial Processes - Wiley Online Library, [online] Available from: <https://onlinelibrary.wiley.com/doi/full/10.1002/ppp.733> (Accessed 12 November 2018), 2011.
- 25 Farbot, H., Isaksen, K., Etzelmüller, B. and Gislås, K.: Ground Thermal Regime and Permafrost Distribution under a Changing Climate in Northern Norway, [online] Available from: <https://onlinelibrary.wiley.com/doi/full/10.1002/ppp.1763> (Accessed 12 November 2018), 2013.
- Fischer, L., Kääh, A., Huggel, C. and Noetzi, J.: Geology, glacier retreat and permafrost degradation as controlling factors of slope instabilities in a high-mountain rock wall: the Monte Rosa east face, *Natural Hazards and Earth System Sciences*, 6(5), 761–772, doi:<https://doi.org/10.5194/nhess-6-761-2006>, 2006.
- 30 Fischer, L., Amann, F., Moore, J. R. and Huggel, C.: Assessment of periglacial slope stability for the 1988 Tschierwa rock avalanche (Piz Morteratsch, Switzerland), *Eng Geol*, 116(1–2), 32–43, doi:10.1016/j.enggeo.2010.07.005, 2010.
- 35 Frauenfelder, R., Isaksen, K., Lato, M. J. and Noetzi, J.: Ground thermal and geomechanical conditions in a permafrost-affected high-latitude rock avalanche site (Polvartinden, northern Norway), *The Cryosphere*, 12(4), 1531–1550, doi:<https://doi.org/10.5194/tc-12-1531-2018>, 2018.
- Furseth, A.: *Skredulykker i Norge*, Tun Forlag, Oslo, Norway, 207 pp, 2006.
- Gareth, J. Witten, D., Hastie, T., and Tibshirani, R.: *An Introduction to Statistical Learning: With Applications in R*. Springer Publishing Company, Incorporated, 426 p, 2014.
- 40 Gislås, K., Etzelmüller, B., Schuler, T. V. and Westermann, S.: CryoGRID 1.0: Permafrost Distribution in Norway estimated by a Spatial Numerical Model, [online] Available from: <https://onlinelibrary.wiley.com/doi/full/10.1002/ppp.1765> (Accessed 12 November 2018), 2013.
- Gislås, K., Westermann, S., Schuler, T. V., Melvold, K., Etzelmüller, B.: Small scale variation of snow in a regional permafrost model, *The Cryosphere*, 10, 1201–1215, DOI:10.5194/tc-10-1201-2016, 2016.
- 45 Gislås, K., Etzelmüller, B., Lussana, C., Hjort, J., Sannel, A. B. K., Isaksen, K., Westermann, S., Kuhry, P., Christiansen, H. H., Frampton, A. and Åkerman, J.: Permafrost Map for Norway, Sweden and Finland, *Permafrost and Periglacial Processes*, 28(2), 359–378, doi:10.1002/ppp.1922, 2017.

- Gruber, S. and Haeberli, W.: Mountain Permafrost. In *Permafrost soils*, pp. 33–44, doi :10.1007/978-3-540-69371-0, 2009.
- 5 Gruber, S., Hoelzle, M. and Haeberli, W.: Permafrost thaw and destabilization of Alpine rock walls in the hot summer of 2003 - Gruber - 2004 - Geophysical Research Letters - Wiley Online Library, [online] Available from: <https://agupubs.onlinelibrary.wiley.com/doi/full/10.1029/2004GL020051> (Accessed 12 November 2018a), 2004a.
- Gruber, S., Hoelzle, M. and Haeberli, W.: Rock-wall temperatures in the Alps: modelling their topographic distribution and regional differences, *Permafrost and Periglacial Processes*, 15(3), 299–307, doi:10.1002/ppp.501, 2004b.
- 10 Haberkorn, A., Phillips, M., Kenner, R., Rhyner, H., Bavay, M., Galos, S. P. and Hoelzle, M.: Thermal regime of rock and its relation to snow cover in steep alpine rock walls: Gemsstock, Central Swiss Alps, *Geografiska Annaler Series A: Physical Geography*, 97(3), 579–597, doi:10.1111/geoa.12101, 2015.
- Haberkorn, A., Wever, N., Hoelzle, M., Phillips, M., Kenner, R., Bavay, M., and Lehning, M.: Distributed snow and rock temperature modelling in steep rock walls using Alpine3D, *The Cryosphere*, 11, 585–607, <https://doi.org/10.5194/tc-11-585-2017>, 2017.
- 15 Haeberli, W. Die Basis-Temperatur der winter-lichen Schneedecke als möglicher Indikator für die Verbreitung von Permafrost in den Alpen. *Zeitschrift für Gletscherkunde und Glazialgeologie*, 9, 221–227, 1973.
- Haeberli, W., Huggel, C., Käab, A., Zraggen-Oswald, S., Polkvoj, A., Galushkin, I., Zotikov, I. and Osokin, N.: The Kolka-Karmadon rock/ice slide of 20 September 2002: an extraordinary event of historical dimensions in North Ossetia, Russian Caucasus, *Journal of Glaciology*, 50(171), 533–546, doi:10.3189/172756504781829710, 2004.
- 20 Hales, T. C., and Roering, J. J.: Climatic controls on frost cracking and implications for the evolution of bedrock landscapes. *Journal of Geophysical Research: Earth Surface*, 112(F2), 2007.
- Hallet, B., J. Walder, and Stubbs, C. W.: Weathering by segregation ice growth in microcracks at sustained sub-zero temperatures: Verification from an experimental study using acoustic emissions, *Permafrost Periglacial Processes*, 2, 283–300, 1991.
- 25 Hanson, S. and Hoelzle, M.: The thermal regime of the active layer at the Murtèl rock glacier based on data from 2002, *Permafrost and Periglacial Processes*, 15(3), 273–282, doi:10.1002/ppp.499, 2004.
- Harris, C., Haeberli, W., Mühl, D. V. and King, L.: Permafrost monitoring in the high mountains of Europe: the PACE Project in its global context, *Permafrost and Periglacial Processes*, 12(1), 3–11, doi:10.1002/ppp.377, 2001.
- 30 Hasler, A., Gruber, S., Font, M. and Dubois, A.: Advective Heat Transport in Frozen Rock Clefts: Conceptual Model, Laboratory Experiments and Numerical Simulation, *Permafrost and Periglacial Processes*, 22(4), 378–389, doi:10.1002/ppp.737, 2011a.
- 35 Hasler, A., Gruber, S. and Haeberli, W.: Temperature variability and offset in steep alpine rock and ice faces, *The Cryosphere*, 5(4), 977–988, doi:10.5194/tc-5-977-2011, 2011b.
- Hasler, A., Geertsema, M., Foord, V., Gruber, S. and Noetzi, J.: The influence of surface characteristics, topography and continentality on mountain permafrost in British Columbia, *The Cryosphere*, 9(3), 1025–1038, doi:<https://doi.org/10.5194/tc-9-1025-2015>, 2015.
- 40 Heggem, E. S., Juliussen, H. and Etzelmüller, B.: Mountain permafrost in Central-Eastern Norway, *Norsk Geografisk Tidsskrift - Norwegian Journal of Geography*, 59(2), 94–108, doi:10.1080/00291950510038377, 2005.
- Hermanns, R., Hansen, L., Sletten, K., Böhme, M., Bunkholt, H., Dehls, J., Eilertsen, R., Fischer, L., L'Heureux, J.-S., Høgaas, F., Nordahl, B., Oppikofer, T., Rubensdotter, L., Solberg, I.-L., Stalsberg, K., and Molina, F. X. Y.: Systematic geological mapping for landslide understanding in the Norwegian context, *Landslide and*
- 45

engineered slopes: protecting society through improved understanding, Taylor & Francis Group, London: 265-271, 2012.

Hermanns, R.L., Dahle, H., Bjerke, P.L., Crosta, G.B., Anda, E., Blikra, L.H., Saintot, A., Longva, O., Eiken, T.: Rock slide dams in Møre og Romsdal county, Norway: Examples for the hazard and potential of rock slide dams. In: Margottini, C., Canuti, P., Sassa, K. (eds): *Landslide science and practice*, 6: Risk Assessment, Management and Mitigation, Springer-Verlag, Berlin Heidelberg, Germany, 3-12, DOI 10.1007/978-3-642-31325-6_1, 2013.

Hermanns, R.L., Oppikofer, T., Roberts, N.J., and Sandøy, G.: Catalogue of historical displacement waves and landslide-triggered tsunamis in Norway, *Engineering Geology for Society and Territory*-Volume 4, Springer, 63-66, ISBN 3319086596, 2014.

Hermanns, R. L., Schleier, M., Bohme, M., Blikra, L. H., Gosse, J., Ivy-Ochs, S., Hilger, P.: Rock-avalanche activity in W and S Norway peaks after the retreat of the Scandinavian Ice Sheet. In: Mikoš M, Vilimek V, Yin Y et al. (eds) *Advancing Culture of Living with Landslides*. Cham: Springer, pp. 331–338, 2017.

Hipp, T., Etzelmüller, B., Farbrot, H. and Schuler, T. V.: *Modelling the temperature evolution of permafrost and seasonal frost in southern Norway during the 20th and 21st century*, *The Cryosphere Discussions*, 5(2), 811–854, doi:<https://doi.org/10.5194/tcd-5-811-2011>, 2011.

Hipp, T., Etzelmüller, B., Farbrot, H., Schuler, T. V. and Westermann, S.: Modelling borehole temperatures in Southern Norway – insights into permafrost dynamics during the 20th and 21st century, *The Cryosphere*, 6(3), 553–571, doi:<https://doi.org/10.5194/tc-6-553-2012>, 2012.

Hipp, T., Etzelmüller, B. and Westermann, S.: Permafrost in Alpine Rock Faces from Jotunheimen and Hurrungane, Southern Norway, *Permafrost and Periglacial Processes*, 25(1), 1–13, doi:10.1002/ppp.1799, 2014.

Hilger, P., Hermanns, R. L., Gosse, J. C., Jacobs, B., Etzelmüller, B., Krautblatter, M.: Multiple rock-slope failures from Mannen in Romsdal Valley, western Norway, revealed from Quaternary geological mapping and 10Be exposure dating, *The Holocene*: 0959683618798165, 2018.

Huggel, C., Zraggen-Oswald, S., Haeberli, W., Kääh, A., Polkvoj, A., Galushkin, I. and Evans, S. G.: The 2002 rock/ice avalanche at Kolka/Karmadon, Russian Caucasus: assessment of extraordinary avalanche formation and mobility, and application of QuickBird satellite imagery, *Natural Hazards and Earth System Sciences*, 5(2), 173–187, doi:<https://doi.org/10.5194/nhess-5-173-2005>, 2005.

Huggel, C., Allen, S., Deline, P., Fischer, L., Noetzli, J. and Ravel, L.: Ice thawing, mountains falling—are alpine rock slope failures increasing?, *Geology Today*, 28(3), 98–104, doi:10.1111/j.1365-2451.2012.00836.x, 2012.

Hughes, A. L. C., Gyllenreutz, R., Lohne, Ø. S., Mangerud, J., Svendsen, J. I.: *The last Eurasian ice sheets—a chronological database and time-slice reconstruction*, *Boreas*, 45, 1–45, doi:10.1111/bor.12142, 2016

Isaksen, K., Hauck, C., Gudevang, E., Ødegård, R. S. and Sollid, J. L.: Mountain permafrost distribution in Dovrefjell and Jotunheimen, southern Norway, based on BTS and DC resistivity tomography data, *Norsk Geografisk Tidsskrift - Norwegian Journal of Geography*, 56(2), 122–136, doi:10.1080/002919502760056459, 2002.

Isaksen, K., Farbrot, H., Blikra, L. H. Johansen, B., and Sollid, J. L.: Five-year ground surface temperature measurements in Finnmark, northern Norway, *Proceedings of the Ninth International Conference on Permafrost*, edited by: Kane, D. L. and Hinkel, K. M., Institute of Northern Engineering, University of Alaska Fairbanks, Fairbanks, Alaska, USA, 789–794, 2008.

Isaksen, K., Ødegård, R. S., Etzelmüller, B., Hilbich, C., Hauck, C., Farbrot, H., Eiken, T., Hygen, H. O. and Hipp, T. F.: Degrading Mountain Permafrost in Southern Norway: Spatial and Temporal Variability of Mean Ground Temperatures, 1999–2009, *Permafrost and Periglacial Processes*, 22(4), 361–377, doi:10.1002/ppp.728, 2011.

IPCC, 2013. Climate Change 2013: The Physical Science Basis. Contribution of Working Group I to the Fifth Assessment Report of the Intergovernmental Panel on Climate Change. Cambridge University Press, Cambridge, United Kingdom and New York, NY, USA, 1535 pp.

- Juliussen, H. and Humlum, O.: Thermal regime of openwork block fields on the mountains Elgâhogna and Sølén, central-eastern Norway, *Permafrost and Periglacial Processes*, 19(1), 1–18, doi:10.1002/ppp.607, 2008.
- Kellerer-Pirklbauer, A.: Potential weathering by freeze-thaw action in alpine rocks in the European Alps during a nine year monitoring period, *Geomorphology*, 296, 113–131, doi:10.1016/j.geomorph.2017.08.020, 2017.
- 5 King, L. High mountain permafrost in Scandinavia, 4th International Conference on Permafrost, Proceedings, National Academy Press, Washington, DC, 612-617, 1983.
- King, L.: Zonation and ecology of high mountain permafrost in Scandinavia, *Geografiska Annaler Series A: Physical Geography*, 68, 131-139, 1986.
- 10 Kleman, J., and Hättetrand, C.: Frozen-bed Fennoscandian and Laurentide ice sheets during the Last Glacial Maximum: *Nature*, 402, 63-66, 1999.
- Kleman, J., Stroeve, A.P., Lundqvist, J.: Patterns of Quaternary ice sheet erosion and deposition in Fennoscandia and a theoretical framework for explanation, *Geomorphology*, 97 (1–2), 73–90, 2008.
- Korup, O.: Linking landslides, hillslope erosion, and landscape evolution, *Earth Surface Processes and Landforms*, 34(9), 1315–1317, doi:10.1002/esp.1830, 2009.
- 15 Krautblatter, M., Funk, D. and Günzel, F. K.: Why permafrost rocks become unstable: a rock–ice-mechanical model in time and space - Krautblatter - 2013 - *Earth Surface Processes and Landforms* - Wiley Online Library, [online] Available from: <https://onlinelibrary.wiley.com/doi/full/10.1002/esp.3374> (Accessed 12 November 2018), 2013.
- 20 Lilleøren, K. S., Etzel Müller, B.: A regional inventory of rock glaciers and ice-cored moraines in Norway, *Geografiska Annaler. Series A, Physical Geography* 93: 175–191. DOI:10.1111/j.1468-0459.2011.00430.x, 2011.
- Lussana, C., Tveito, O. E. and Uboldi, F.: Three-dimensional spatial interpolation of 2 m temperature over Norway, *Quarterly Journal of the Royal Meteorological Society*, 144(711), 344–364, doi:10.1002/qj.3208, 2017.
- 25 Magnin, F., Deline, P., Ravanel, L., Noetzi, J. and Pogliotti, P.: Thermal characteristics of permafrost in the steep alpine rock walls of the Aiguille du Midi (Mont Blanc Massif, 3842 m a.s.l.), *The Cryosphere*, 9(1), 109–121, doi:https://doi.org/10.5194/tc-9-109-2015, 2015a.
- Magnin, F., Brenning, A., Bodin, X., Deline, P. and Ravanel, L.: Modélisation statistique de la distribution du permafrost de paroi : application au massif du Mont Blanc, *Géomorphologie : relief, processus, environnement*, 21(vol. 21 – n° 2), 145–162, doi:10.4000/geomorphologie.10965, 2015b.
- 30 Magnin, F., Westermann, S., Pogliotti, P., Ravanel, L., Deline, P. and Malet, E.: Snow control on active layer thickness in steep alpine rock walls (Aiguille du Midi, 3842 m a.s.l., Mont Blanc massif), *CATENA*, 149, p648–p662, 2017a.
- 35 Magnin, F., Josnin, J.-Y., Ravanel, L., Pergaud, J., Pohl, B. and Deline, P.: Modelling rock wall permafrost degradation in the Mont Blanc massif from the LIA to the end of the 21st century, *The Cryosphere*, 11(4), 1813–1834, doi:https://doi.org/10.5194/tc-11-1813-2017, 2017a2017b.
- Mamot, P., Weber, S., Schröder, T. and Krautblatter, M.: A temperature- and stress-controlled failure criterion for ice-filled permafrost rock joints, *The Cryosphere*, 12(10), 3333–3353, doi:10.5194/tc-12-3333-2018, 2018.
- McColl S.T., Paraglacial rock-slope stability, *Geomorphology*, 153-154, 1-16, 2012.
- 40 Magnin, F., Westermann, S., Pogliotti, P., Ravanel, L., Deline, P. and Malet, E.: Snow control on active layer thickness in steep alpine rock walls (Aiguille du Midi, 3842 m a.s.l., Mont Blanc massif), *CATENA*, 149, p648–p662, 2017b.
- Matsuoka, N. and Murton, J.: Frost weathering: recent advances and future directions, *Permafrost and Periglacial Processes*, 19(2), 195–210, doi:10.1002/ppp.620, 2008.

- Myhra, K. S., Westermann, S. and Etzelmüller, B.: Modelled Distribution and Temporal Evolution of Permafrost in Steep Rock Walls Along a Latitudinal Transect in Norway by CryoGrid 2D, *Permafrost and Periglacial Processes*, 28(1), 172–182, doi:10.1002/ppp.1884, 2017.
- 5 Noetzli, J. and Gruber, S.: Transient thermal effects in Alpine permafrost, *The Cryosphere*, 3(1), 85–99, doi:10.5194/tc-3-85-2009, 2009.
- Noetzli, J., Gruber, S., Kohl, T., Salzmann, N. and Haeberli, W.: [Three-dimensional distribution and evolution of permafrost temperatures in idealized high-mountain topography](#), *Journal of Geophysical Research: Earth Surface*, 112(F2), doi:10.1029/2006JF000545, 2007.
- 10 Ødegård, R. S., Sollid, J. L. and Liestøl, O.: Ground temperature measurements in mountain permafrost, Jotunheimen, southern Norway, *Permafrost and Periglacial Processes*, 3(3), 231–234, doi:10.1002/ppp.3430030310, 1992.
- Oppikofer, T., Nordahl, B., Bunkholt, H., Nicolaisen, M., Jarna, A., Iversen, S., Hermanns, R. L., Böhme, M. and Yugi Molina, F. X.: Database and online map service on unstable rock slopes in Norway — From data perpetuation to public information, *Geomorphology*, 249, 69–81, doi:10.1016/j.geomorph.2015.08.005, 2015.
- 15 [R Core Team. : R: A language and environment for statistical computing. R Foundation for Statistical Computing, Vienna, Austria, 2013.](#)
- Ravanel, L., Magnin, F. and Deline, P.: Impacts of the 2003 and 2015 summer heatwaves on permafrost-affected rock-walls in the Mont Blanc massif, *Science of The Total Environment*, 609, 132–143, doi:10.1016/j.scitotenv.2017.07.055, 2017.
- 20 Romstad, B., Harbitz, C. B. and Domaas, U.: A GIS method for assessment of rock slide tsunami hazard in Norwegian lakes and reservoirs, *Natural hazards and earth system sciences*, 9(2), 353–364, doi:http://dx.doi.org/10.5194/nhess-9-353-2009, 2009.
- 25 [Sattler, K., Anderson, B., Mackintosh, A., Norton, K. and de Róiste, M.: Estimating Permafrost Distribution in the Maritime Southern Alps, New Zealand, Based on Climatic Conditions at Rock Glacier Sites, *Front. Earth Sci.*, 4, doi:10.3389/feart.2016.00004, 2016.](#)
- [Savi, S., Delunel, R., Schlunegger, F.: Efficiency of frost-cracking processes through space and time: An example from the eastern Italian Alps. *Geomorphology*, 232: 248-260. 10.1016/j.geomorph.2015.01.009, 2015.](#)
- 30 Sellier, D.: Le felsenmeer du Mont Gausta (Telemark, Norvège) : environnement, caractères morphologiques et significations paléogéographiques, *Géographie physique et Quaternaire*, 49(2), 185–205. doi:10.7202/033036ar, 1995.
- 35 [Sollid, J. L., & Sørbel, L. Palsa bogs as a climate indicator: examples from Dovrefjell, southern Norway. *Ambio*, 287-291, 1998.](#)
- Sollid, J., Isaksen, K., Eiken, T., and Ødegård, R.: The transition zone of mountain permafrost on Dovrefjell, southern Norway, in: *Proceedings of the International Conference on Permafrost*, 2, 1085–1090, 2003.
- Sosio, R., Crosta, G. B. and Hungr, O.: Complete dynamic modeling calibration for the Thurwieser rock avalanche (Italian Central Alps), *Engineering Geology*, 100(1), 11–26, doi:10.1016/j.enggeo.2008.02.012, 2008.
- 40 Steiger, C., Etzelmüller, B., Westermann, S. and Myhra, K. S.: Modelling the permafrost distribution in steep rock walls, *Norwegian Journal of Geology*, doi:10.17850/njg96-4-04, 2016.
- Westermann, S., Schuler, T. V., Gislås, K. and Etzelmüller, B.: Transient thermal modeling of permafrost conditions in Southern Norway, *The Cryosphere*, 7(2), 719–739, doi:10.5194/tc-7-719-2013, 2013.

Figures

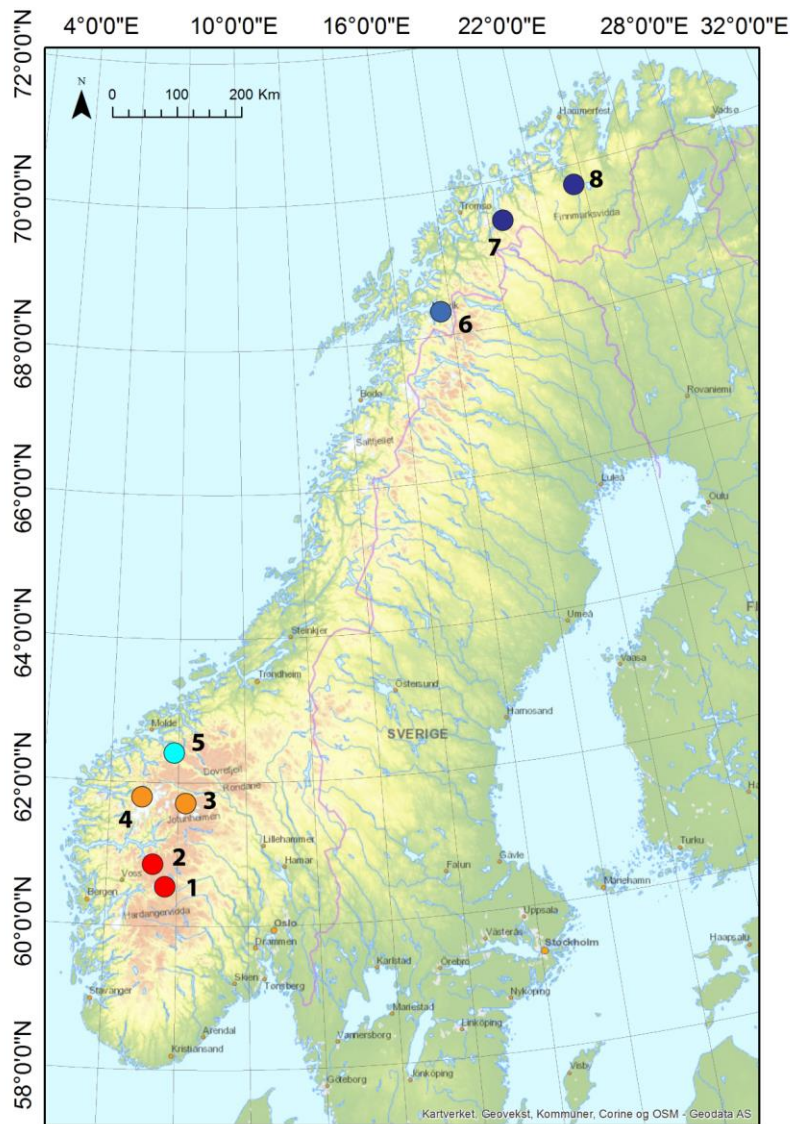


Figure 1. Location of the rock surface temperature loggers in steep rock slopes across Norway. **1.** Finse (1 logger). **2.** Flåm (3 loggers). **3.** Jotunheimen (4 loggers). **4.** Loe (3 loggers). **5.** Mannen (2 loggers). **6.** Narvik (3 loggers). **7.** Kåfjord (7 loggers). **8.** Alta (2 loggers). The color range is adapted to latitude in accordance with Figure 2.

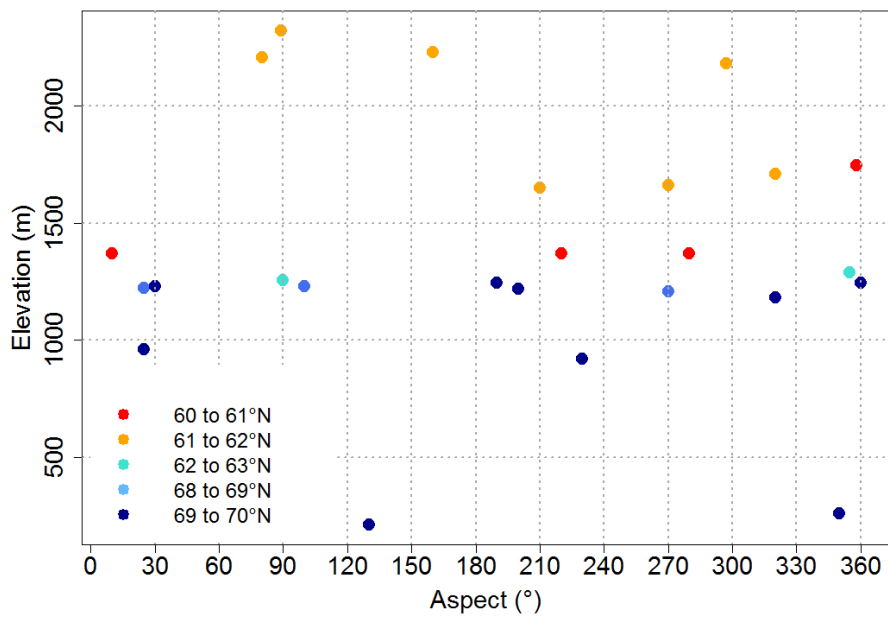


Figure 2. Distribution of the 25 loggers according to elevation, aspect and latitude.

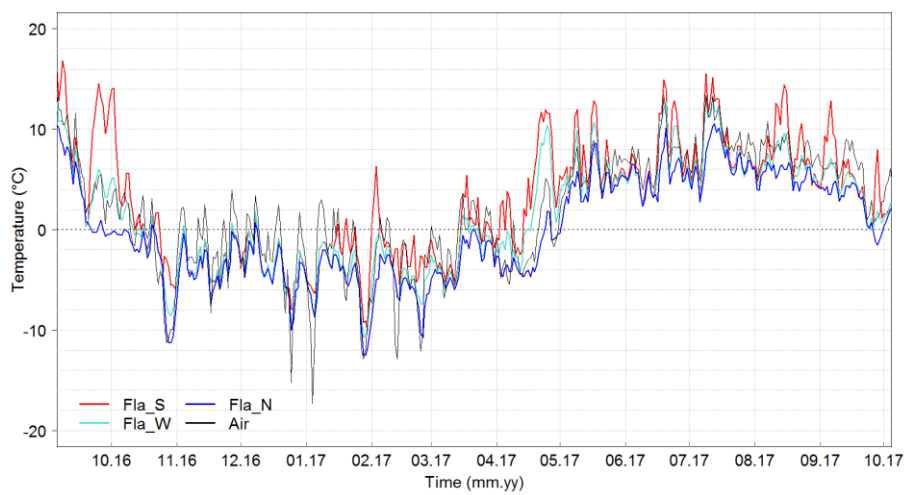


Figure 3. Example of daily rock surface temperature data for the site of Flâm during one hydrological year.

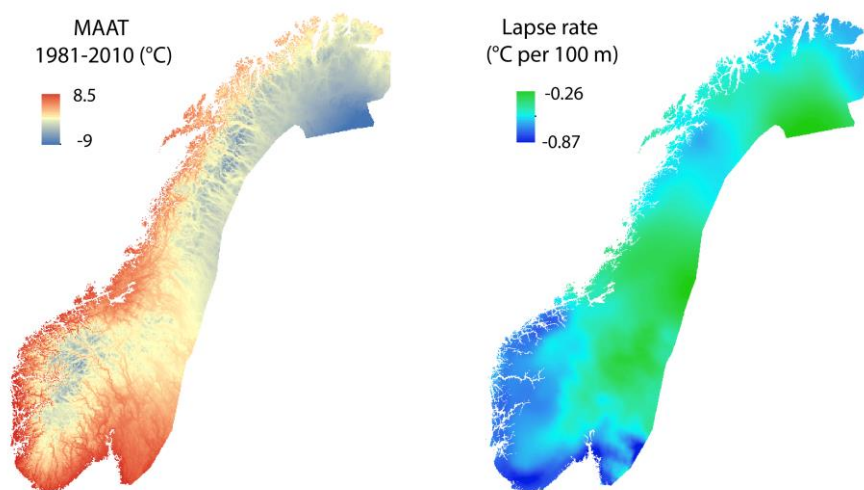


Figure 4. 1km grid Mean Annual Air Temperature (MAAT) derived from the SeNorge2 dataset (left, Lussana et al., 2017) and averaged lapse rate over a 25 km radius (right).

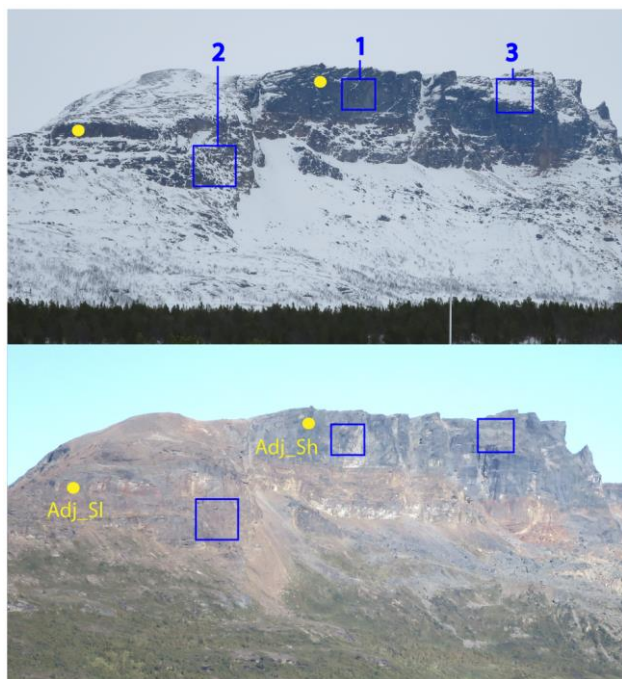
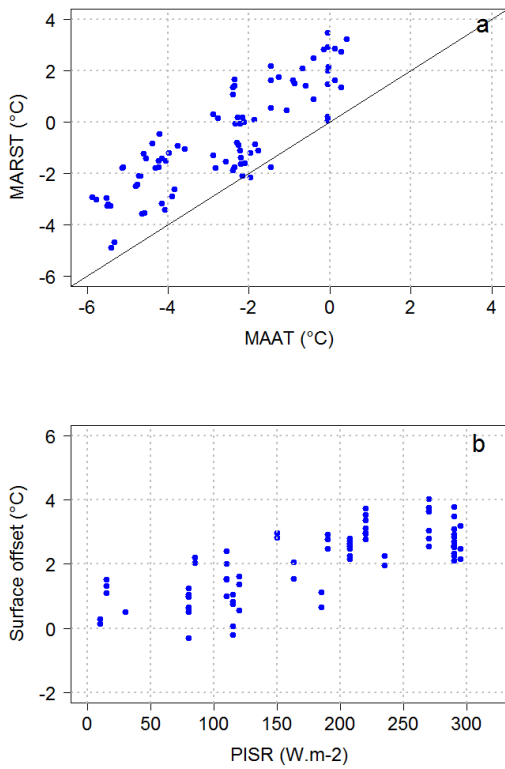


Figure 5. Pictures of the Ádjit crest (top: March 2017, bottom: August 2018) showing variable bedrock settings more or less favorable to permafrost occurrence. 1. Vertical and compact bedrock. 2. ~~Rugged Fractured~~-bedrock

surface and with sparse snow deposits. 3. Highly-fractured-Mid-steep slope with substantial snow and debris accumulations. Yellow dots indicate logger locations.



5 **Figure 6. a.** Measured Mean Annual Rock Surface Temperature (MARST) *versus* interpolated MAAT at the MARST measurement points. **b.** Surface offset (*i.e.* MARST measured – MAAT interpolated) *versus* calculated Potential Incoming Solar Radiation (PISR) at measurement points. The multiple MARST points for a same PISR values result of the multiple years of RST records at a same logger, and for which the PISR value remains identical.

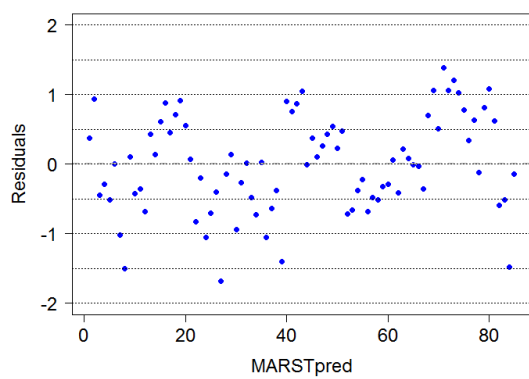


Figure 7. Residuals of the predicted MARST.

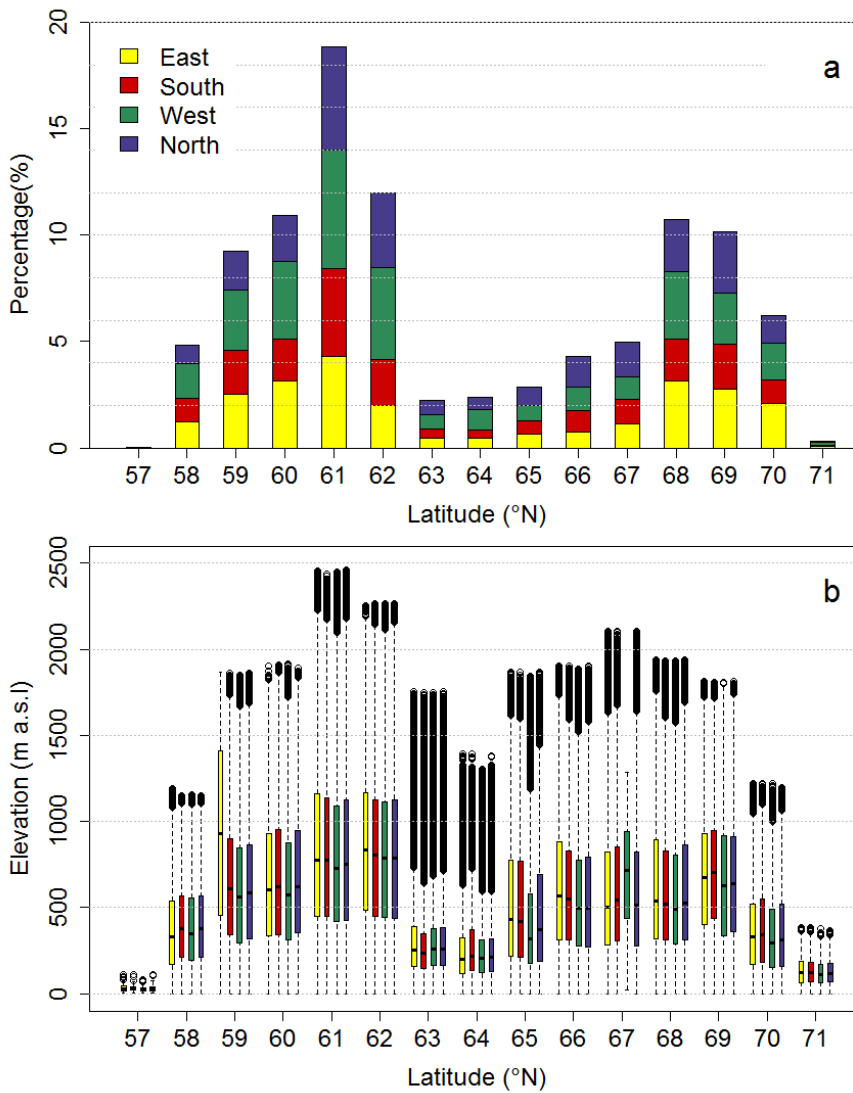


Figure 8. Relative distribution of steep rock walls across Norway (slopes $> 40^\circ$ based on the 10 m resolution DEM). **a.** Relative distribution of rock wall surface area according to aspect and latitude. **b.** Relative distribution of rock wall according to latitude and aspect and elevation. East: 45 to 135° ; South: 135 to 225° ; West: 225 to 315° ; North: 315 to 45° .

The lowest and highest boundaries of the boxes respectively display the 1st and 3rd quartile (Q1 and Q3) of the observations. The lowest and highest whiskers respectively show $Q1 - ((Q3 - Q1) \times 1.5)$ and $(Q3 + ((Q3 - Q1) \times 1.5))$. The dots are the outliers.

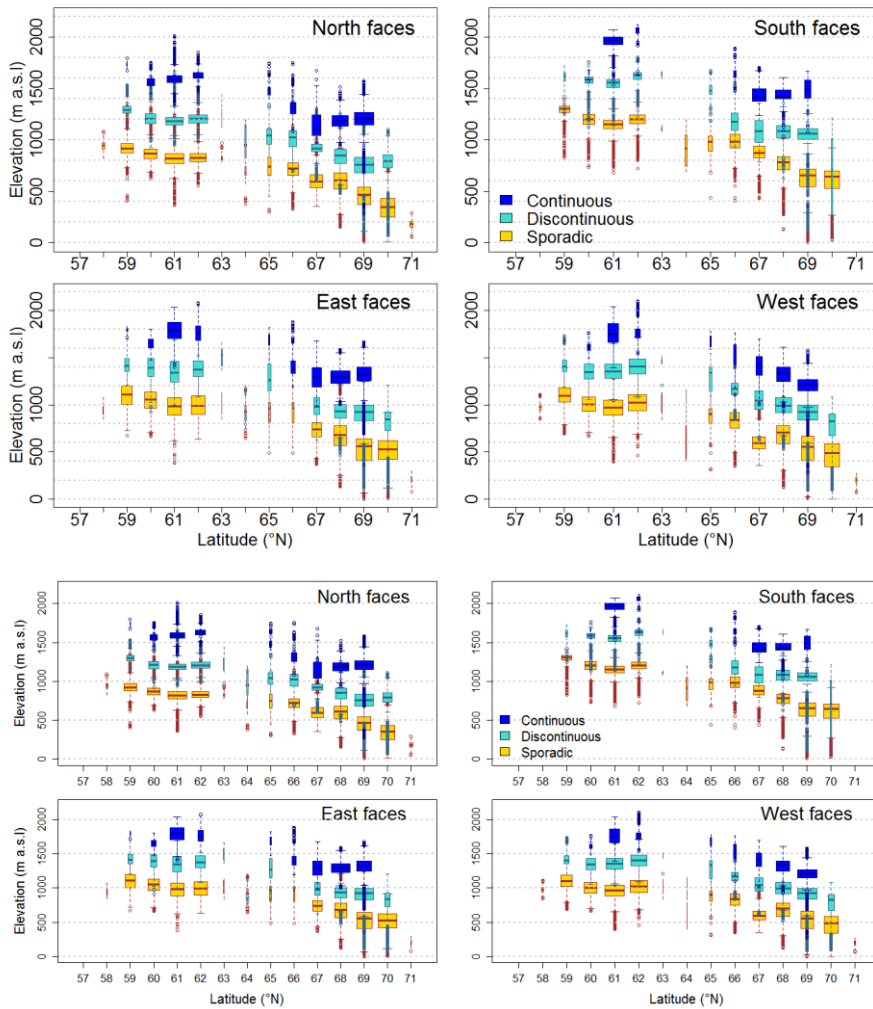


Figure 9. Distribution of the lower limit of each permafrost class according to elevation, aspect and latitude. The width of the boxes is proportional to the square-roots of the number of observations in the respective groups. The lowest and highest boundaries of the boxes respectively display the 1st and 3rd quartile (Q1 and Q3) of the observations. The lowest and highest whiskers respectively show $Q1 - ((Q3 - Q1) \times 1.5)$ and $Q3 + ((Q3 - Q1) \times 1.5)$. The dots are the outliers.

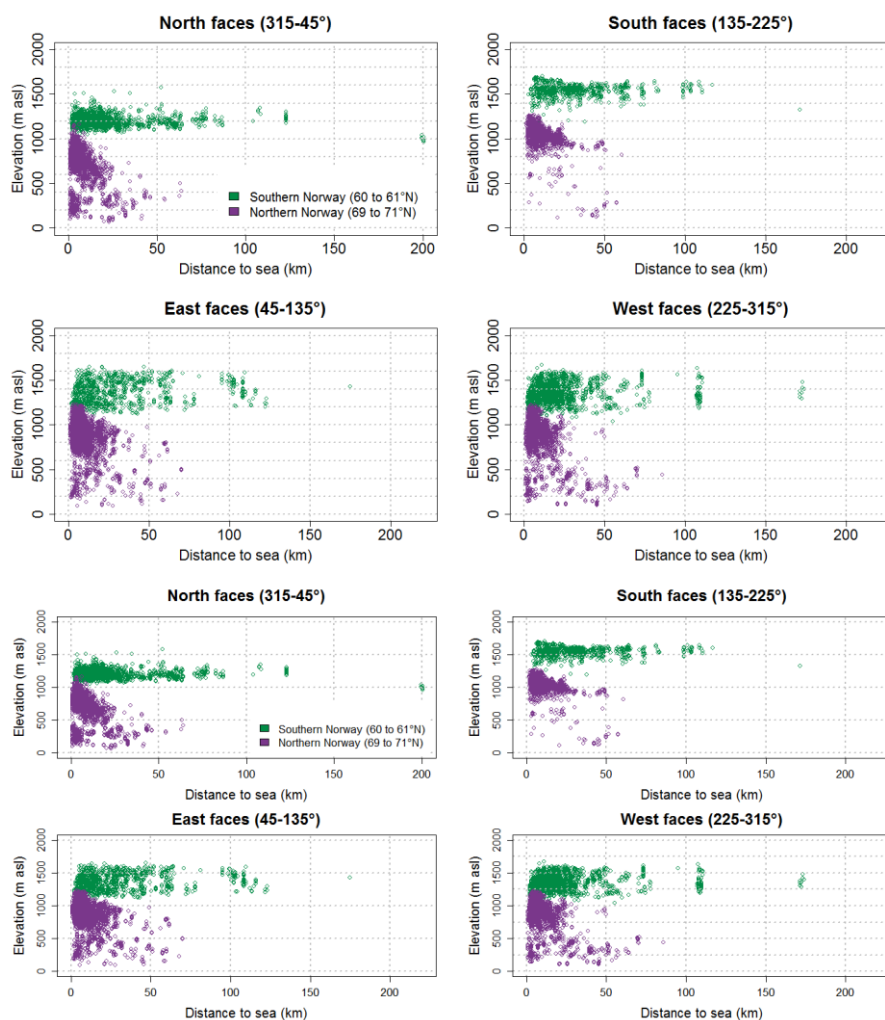


Figure 10. Distribution of the lower limit of discontinuous permafrost in Southern and Northern Norway according the distance to the sea.

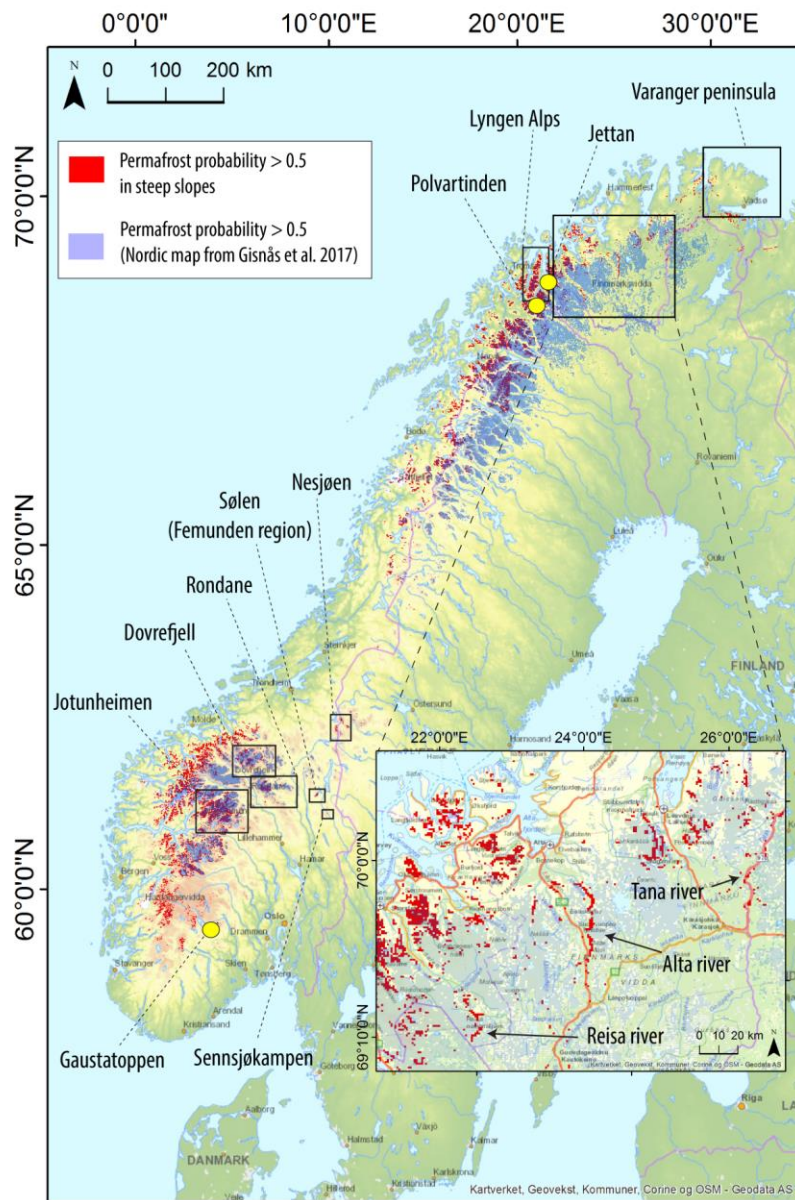
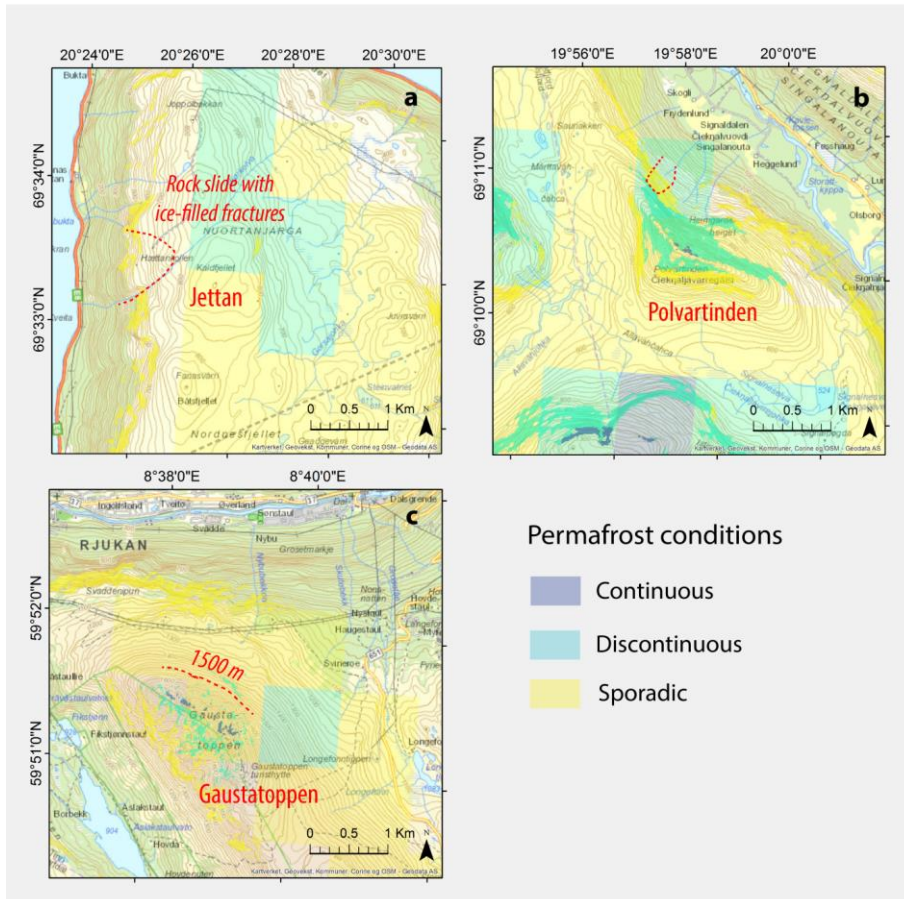


Figure 11. Permafrost distribution in steep rock slopes of Norway according to the CryoWall map and in Scandinavia according to the map produced by Gissnäs et al. (2017). For steep rock slopes permafrost, only the discontinuous and continuous permafrost classes are displayed as the lower limit of discontinuous permafrost corresponds to the isotherm 0°C and cover the main permafrost areas. Areas of interest for the discussion are displayed.



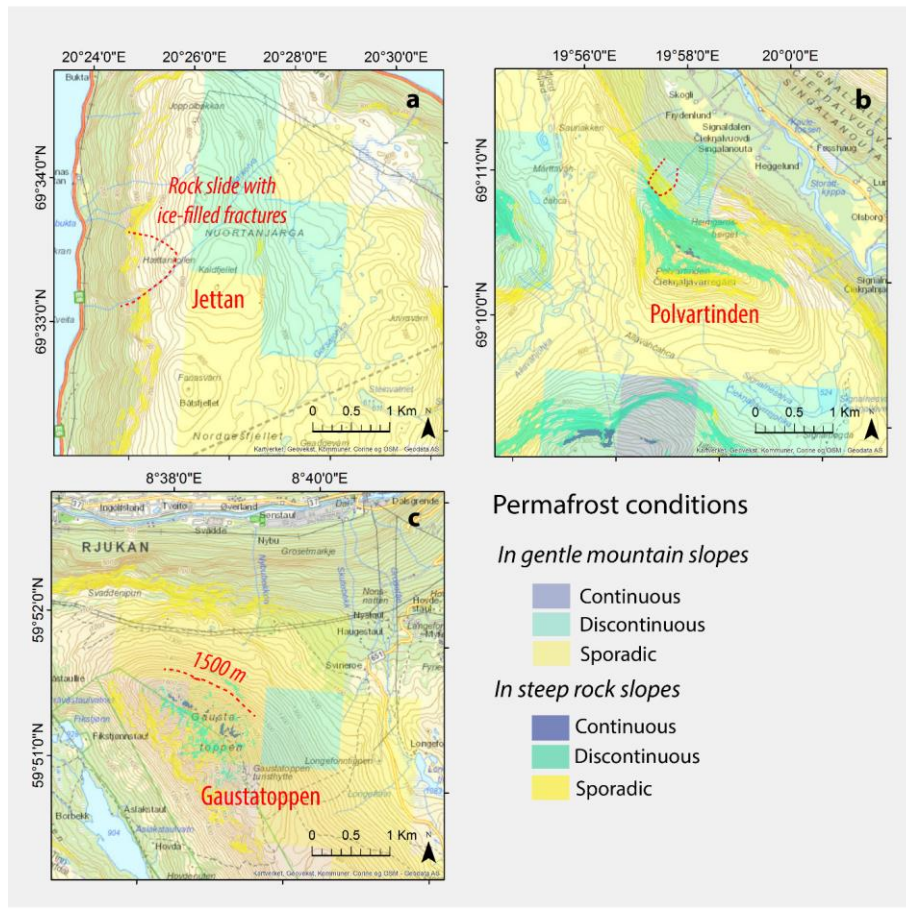


Figure 12. Permafrost distribution at steep slope sites where permafrost has been previously observed in Norway (a. Blikra and Christiansen, 2014; b. Frauenfelder et al., 2018; c. Etzelmueller et al., 2003b). The CryoWall map has been combined with the 1 km resolution Nordic permafrost map (Gisnås et al., 2017) to display predicted permafrost in all types of terrains.

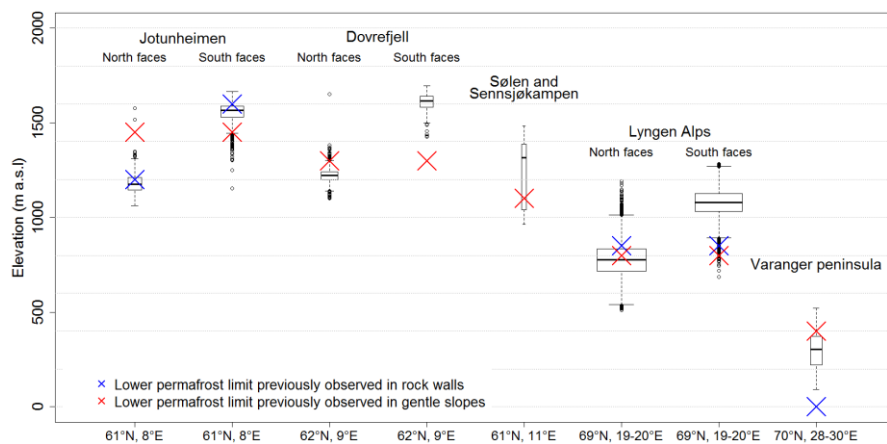


Figure 13. Comparison of steep slopes permafrost distribution in specific regions with estimations from previous studies (Hipp et al., 2014; Isaksen et al., 2002; 2008; 2011; Farbrot et al., 2011; 2013; Sollid et al., 2003; Westermann et al., 2013; Heggem et al., 2005; Steiger et al., 2016; Gislås et al., 2017; Borge et al., 2017). The width of the boxes is proportional to the square-roots of the number of observations in the respective groups.

5

Tables

Area	ID	Latitude, Longitude	Elevation (m asl)	Aspect (°)	Date of installation
(1) Finse	Fin_N	60°33'25.6"N, 7°27'40.2"E	1743	358	23.09.2017
	Fla_S	60° 50' 35.9"N, 7° 9' 52.7"E	1370	220	11.08.2016
(2) Flåm	Fla_N	60° 50' 41.1"N, 7° 9' 47.2"E	1370	10	11.08.2016
	Fla_W	60° 50' 40.6"N, 7° 9' 46.8"E	1370	280	11.08.2016
(3) Jotun- heimen	Juv_El	61°39'12.4" N 8°19'36.6"E	2204	82	26.09.2010
	Juv_S	61° 39' 0.7" N 8° 18' 43.9"E	2226	162	26.09.2010
	Juv_W	61° 38' 48.4" N 8° 18' 32.1"E	2179	297	27.09.2010
	Juv_Eh	61° 38' 27.4" N 8° 18' 22.4"E	2320	89	27.09.2010
	Loe_S	61° 49' 32.0" N 7° 1' 20.5"E	1648	210	13.08.2015
(4) Loen	Loe_W	61° 49' 32.4" N 7° 1' 27.3"E	1662	270	13.08.2015
	Loe_N	61° 49' 17.3"N, 7° 1' 48.7"E	1709	320	13.08.2015
(5) Mannen	Man_E	62° 27' 21.5"N, 7° 46' 45.0"E	1290	90	06.08.2015
	Man_N	62° 27' 21.4"N, 7° 46' 45.2"E	1290	350	06.08.2015
(6) Narvik	Nar_N	68° 26' 1.8" N, 17° 34' 49.9"E	1224	25	29.08.2016
	Nar_E	68° 26' 1.5" N, 17° 34' 50.3"E	1228	100	29.08.2016
	Nar_W	68° 26' 3.0" N, 17° 34' 40.9"E	1208	270	29.08.2016
	Anka_N	69° 28' 34.7" N, 20° 29' 30.2"E	960	25	25.08.2015
(7) Kåfjord	Gam_S	69° 28' 53.5" N, 20° 34' 28.1"E	1220	200	25.08.2015
	Gam_W	69° 28' 53.6" N, 20° 34' 28.2"E	1183	320	25.08.2015
	Gam_N	69° 28' 59.3" N, 20° 34' 42.0"E	1243	360	25.08.2015
	Adj_Sl	69° 22' 25.2" N, 20° 23' 25.3"E	920	230	24.08.2015
	Adj_Sh	69° 22' 3.5" N, 20° 25' 20.4"E	1245	190	24.08.2015
	Adj_N	69° 22' 3.2" N, 20° 25' 24.1"E	1230	30	24.08.2015
(8) Alta	Alt_N	69 46' 04.3"N, 23 41'47.0"E	260	350	03.09.2016
	Alt_S	69 46'12.6"N, 23 41'33.7"E	215	130	03.09.2016

Table 1. Settings of the temperature sensors used in this study

ID	Aver. Period*	Nb of days missing for **	Weather station name and elevation– (m asl.) ***	Correlation with RST****
Fin_Nl	NoData	0	-	-
Fin_Nh	25.09. to 24.09	0	-	-
Fla_S	15.08 to 14.08	0	-	-
Fla_N	15.08 to 14.08	0	-	-
Fla_W	15.08 to 14.08	0	-	-
Juv_El	28.09 to 27.09	21	Sogneflehytta (1413)	0.8264
Juv_S	28.09 to 27.09	21	Juvvasshøe (1894)	0.8153
Juv_W	28.09 to 27.09	21	Sogneflehytta (1413)	0.8384
Juv_Eh	28.09 to 27.09	21	Juvvasshøe (1894)	0.7741
Loe_S	15.08 to 14.08	0	-	-
Loe_W	15.08 to 14.08	0	-	-
Loe_N	15.08 to 14.08	0	-	-
Man_E	07.08 to 06.08	6	Mannen (1294)	0.87
Man_N	07.08 to 06.08	6	Mannen (1294)	0.91
Rom_N	30.08 to 29.08	0	-	-
Rom_E	30.08 to 29.08	0	-	-
Rom_W	30.08 to 29.08	0	-	-
Anka_N	01.09 to 31.08	0	-	-
Gam_S	01.09 to 31.08	0	-	-
Gam_W	01.09 to 31.08	0	-	-
Gam_N	01.09 to 31.08	0	-	-
Adj_Sl	01.09 to 31.08	0	-	-
Adj_Sh	01.09 to 31.08	0	-	-
Adj_N	01.09 to 31.08	0	-	-
Alt_N	04.09 to 03.09	4	Alta airport-lufthavn (3)	0.942
Alt_S	04.09 to 03.09	4	Alta airport-lufthavn (3)	0.9109

* Averaging period for the MARST calculation

** Number of days missing for the calculation of the most recent MARST

*** Elevation of the weather station chosen to reconstruct the daily RST during the missing days

**** Correlation between the daily RST and the daily AT recorded at the weather station

Table 2. Summary of the data used for calculating the MARST

ID	Weather stations name, date of installation and elevations (m asl.)	Correlation with RST	Missing data during the period (%)
Fin_Nh	960	0.9398	0
	Midstova, November 2011, 1162	0.9499	
Fla_S		0.7693	
		0.7438	
Fla_N	Klevavatnet, November 2013 (960)	0.9297	0
	Vestredalen, January 2012 (1160)	0.9358	18.2
Fla_W		0.8897	
		0.874	
Juv_El		0.8264	
		0.8103	
Juv_S	Sognefjellhytta, December 1978 (1413)	0.805	
	Juvvasshøytta, September 1999 (1894)	0.8153	
Juv_W		0.8384	0
		0.812	0
Juv_Eh		0.7741	
		0.7444	
Loe_S		0.7504	
		0.7119	
Loe_W	Utvikfjellet, August 2011 (635)	0.7997	21.6
	Trolledalsegga, October 2015 (1020)	0.7676	4.8
Loe_N		0.9422	
		0.915	
Man_E		0.8139	
	Marstein, February 2010 (67)	0.8768	
Man_N	Mannen, March 2010 (1294)	0.8625	0.5
		0.9065	2.6
Rom_N		0.8912	
		0.8835	
Rom_E	Straumsnes, January 2011 (200)	0.8628	0
	Fagernesfjellet, January 1979 (1000)	0.8606	0
Rom_W		0.8836	
		0.8884	
Anka_N		0.872	
		0.8383	
Gam_S		0.8407	
		0.7719	
Gam_W		0.8828	
		0.874	
Gam_N	Skibotn II (20)	0.8452	3.3
	Jettan, July 2015 (691)	0.8458	0
Adj_SI		0.8795	
		0.8521	
Adj_Sh		0.8459	
		0.7712	
Adj_N		0.8898	
		0.8556	
Alt_N		0.942	
	Alta airport lufthavn, December 1963 (3)	0.9241	0
Alt_S	Sihccajavri, April 2013 (382)	0.9109	0
		0.9003	

Table 3. Summary of the data used for the MAAT calculation

	Min	Mean	Median	Max
MARST (°C)	-4.9	-0.6	-1.05	3.5
MAAT (°C)	-5.9	-2.6	-2.4	0.4
PISR (W m⁻²)	10	179	208	295

Table 4. Summary of the model variables

Intercept	0.478*
PISR (Wm^{-2})	0.0097***
MAAT ($^{\circ}\text{C}$)	1.06***
R^2	0.88
R^2_{adj}	0.88
R^2_{cv}	0.88
RMSE ($^{\circ}\text{C}$)	0.63
RMSE_{cv} ($^{\circ}\text{C}$)	0.69
MAE ($^{\circ}\text{C}$)	0.56
MAE_{cv} ($^{\circ}\text{C}$)	0.58
Standard deviation ($^{\circ}\text{C}$)	1.86
Residual standard error ($^{\circ}\text{C}$)	0.699
p-value	< 2.2e-16

Table 5. Summary statistics of the model. Significance of Wald test: *<0.05, ***<0.001